# Generation and Characterization of *Trans*-mitochondrial Mice Carrying mtDNA with a Point Mutation in $tRNA^{Lys}$ Gene

A Dissertation Submitted to
the Graduate School of Life and Environmental Science,
the University of Tsukuba
in Partial Fulfillment of the Requirements
for the Degree of Doctor of Philosophy in Science
(Doctoral Program in Biological Sciences)

Akinori SHIMIZU

# TABLE OF CONTENTS

# ABBREVIATIONS

| | |
|---|---|
| mtDNA | mitochondrial DNA |
| ΔmtDNA | mitochondrial DNA carrying a large-scale deletion |
| CPEO | chronic progressive external ophthalmoplegia |
| MERRF | myoclonic epilepsy with ragged-red fibers |
| MELAS | mitochondrial myopathy, encephalopathy, lactic acidosis, and stroke-like episodes |
| mito-mouse | *trans*-mitochondrial mouse |
| mito-mouse-Δ | *trans*-mitochondrial mouse harboring ΔmtDNA |
| HAT | hypoxanthine–aminopterin–thymidine |
| $\rho^0$ | mtDNA-less |
| BrdU | bromodeoxyuridine |
| B6 | C57BL/6J strain |
| BUN | blood urea nitrogen |
| RRF | ragged-red fiber |
| COX | cytochrome *c* oxidase |
| SDH | succinate dehydrogenase |
| mito-mouse-$tRNA^{Lys7731}$ | *trans*-mitochondrial mouse harboring G7731A mtDNA |
| PGD | preimplantation genetic diagnosis |

# ABSTRACT

I generated *trans*-mitochondrial mice (mito-mice) that carry a mutation in the $tRNA^{Lys}$ gene encoded by mitochondrial DNA (mtDNA) for use in studies of its pathogenesis and transmission profiles. Because patients with mitochondrial diseases frequently carry mutations in the mitochondrial $tRNA^{Lys}$ and $tRNA^{Leu(UUR)}$ genes, I focused my efforts on identifying somatic mutations of these genes in mouse lung carcinoma P29 cells. Of the 43 clones of PCR products including the $tRNA^{Lys}$ or $tRNA^{Leu(UUR)}$ genes in mtDNA of P29 cells, one had a potentially pathogenic mutation (G7731A) in the $tRNA^{Lys}$ gene. P29 subclones with predominant amounts of G7731A mtDNA expressed respiration defects, thus suggesting the pathogenicity of this mutation. I then transferred G7731A mtDNA into mouse ES cells and obtained $F_0$ chimeric mice. Mating these $F_0$ mice with C57BL/6J (B6) male mice resulted in the generation of $F_1$ mice with G7731A mtDNA, named 'mito-mice-$tRNA^{Lys7731}$'. Mito-mice-$tRNA^{Lys7731}$ with high proportions of G7731A mtDNA exclusively expressed respiration defects and disease-related phenotypes, but they expressed only muscle weakness and short body length by four months. I then examined the effects of their aging on metabolic and histologic features. Unlike young mito-mice-$tRNA^{Lys7731}$, aged mito-mice-$tRNA^{Lys7731}$ developed muscle atrophy, renal failures, and various metabolic abnormalities, such as lactic acidosis and anemia, characteristic of patients with mitochondrial diseases. Moreover, the proportion of mutated mtDNA varied markedly among the pups born to each dam, suggesting that selecting oocytes with high proportions of normal mtDNA from affected mothers with $tRNA^{Lys}$-based mitochondrial diseases may be effective as primary prevention for obtaining unaffected children.

# INTRODUCTION

Mitochondrial DNA (mtDNA) carrying a large-scale deletion (ΔmtDNA), single point mutations in the $tRNA^{Lys}$ gene, and in the $tRNA^{Leu(UUR)}$ gene causes CPEO (chronic progressive external ophthalmoplegia), MERRF (myoclonic epilepsy with ragged-red fibers), and MELAS (mitochondrial myopathy, encephalopathy, lactic acidosis, and stroke-like episodes), respectively—the three most prevalent mitochondrial diseases (1-3). However, there are slight differences among the three disease phenotypes, even though these pathogenic mtDNA mutations all induce mitochondrial respiration defects. Considering that mitochondrial respiratory function is controlled by both mitochondrial and nuclear genomes (1-3), this controversial issue can be clarified by generating *trans*-mitochondrial mice ('mito-mice') that share the same nuclear genetic background but carry different pathogenic mtDNA mutations corresponding to the mutations found in the three prevalent mitochondrial diseases. However, no well-established effective protocols are available for introducing mutagenized mtDNA into the mitochondria of mammalian cells.

The previous studies (4-8) showed mtDNAs carrying pathogenic mutations in mouse cell lines, transferred them into mouse female germlines, and generated several types of mito-mice, including mito-mice-Δ (4, 5) which harbor ΔmtDNA and therefore are disease models for CPEO. However, mito-mice harboring mtDNA with pathogenic mutations in the $tRNA^{Lys}$ and $tRNA^{Leu(UUR)}$ genes—and therefore prospective disease models of MERRF and MELAS, respectively—have not previously been established due to the unavailability of mouse cell lines with corresponding tRNA mutations in mtDNA.

To complement the paucity of effective technologies required for introducing mutagenized mtDNA into mitochondria of living mouse cells, I here developed an

alternative strategy involving cloning and sequence analysis to detect small amounts of mtDNA with somatic mutations in the mitochondrial tRNA genes. Because pathogenic mutations responsible for mitochondrial diseases occur preferentially in the $tRNA^{Leu(UUR)}$ and $tRNA^{Lys}$ genes of humans (1-3), I sequenced 43 clones generated from PCR products carrying the mitochondrial $tRNA^{Leu(UUR)}$ and $tRNA^{Lys}$ genes of P29 mouse lung carcinoma cells (9). One of the 43 clones had a somatic G7731A mutation in $tRNA^{Lys}$, which enabled the generation of *trans*-mitochondrial mito-mice expressing respiration defects for their use as models for diseases caused by mutations in the mitochondrial $tRNA^{Lys}$ gene.

# MATERIALS & METHODS

### *Cell lines and cell culture*

Mouse P29 cells, their subclones, mtDNA-less ($\rho^0$) B82 cells, and their *trans*-mitochondrial cybrid clones were grown in DMEM (Sigma-Aldrich, St. Louis, USA) containing 10% fetal calf serum, uridine (50 ng/ml), and pyruvate (100 ng/ml). Mouse ES cells (TT2-F, an XO subline established from XY TT2 cells; Riken Center for Developmental Biology) and *trans*-mitochondrial ES cybrids were cultivated on mitomycin-C–inactivated feeder cells derived from fetal fibroblasts in DMEM (Invitrogen) supplemented with 15% Knockout Serum Replacement (Invitrogen), non-essential amino acids (MP Biomedicals LLC), leukemia inhibitory factor (105 U/ml, Invitrogen), and 100 μM 2-mercaptoethanol (Sigma–Aldrich).

### *Cloning and sequencing of PCR products*

Total DNA extracted from P29 cells was used as the template for PCR amplifications, which generated two mtDNA fragments, F1 and F2, by using unique primer pairs that were designed to generate 2.6- and 2.7-kb fragments, respectively. The sequences of the primers were based on the standard mtDNA sequence of B6 mice (GenBank accession no., AY172335): F1 forward, nucleotides 2045–2064; F1 reverse, 4623–4603; F2 forward, 5931–5950; and F2 reverse, 8626–8606 (Fig. 1). All PCR amplifications were performed in 50 μl of solution consisting of PCR buffer, 0.2 mM dNTPs, 0.6 mM primers, 1 U Ampli*Taq* Gold DNA polymerase (Perkin-Elmer Applied Biosystems), and 1 μg of cellular DNA as template. Reaction conditions were 95 ºC for 10 min, followed by 35 cycles of 60 s at 95 ºC, 60 s at 50–56 ºC, and 150 s at 72 ºC. PCR products were ligated into pUC118 (Takara) and then introduced into DH5α cells (Takara). Sequence templates were prepared by using a TempliPhi DNA Sequencing

Template Amplification Kit (Amersham Pharmacia Biosciences) according to the manufacturer's protocol. Sequence reactions were performed by using dye termination methods (Takara PCR Thermal Cycler GP), and samples were sequenced on a MegaBACE1000 automated sequencer (Amersham Pharmacia Biosciences).

***Genotyping of mtDNA***

To detect the T7728C mutation, a 71-bp fragment containing the 7728 site was PCR-amplified by using the nucleotide sequences 7703 to 7723 (5′-TATGAAGCTAAGAGCGgaAAC-3′, small letters indicate mismatch) and 7773 to 7754 (5′-TGTGGCATATCACTATGGAG-3′) as oligonucleotide primers. Combination of the PCR-generated mutation with the T7728C mutation creates a restriction site for *Xmn*I and generates 50- and 21-bp fragments on *Xmn*I digestion of the PCR products. To detect the G7731A mutation, a 130-bp fragment containing the 7731 site was PCR-amplified by using the nucleotide sequences from 7633 to 7653 (5′-GCCCATTGTCCTAGAAATGGT-3′) and 7762 to 7732 (5′-ACTATGGAGATTTTAAGGTCTCTAACTTTAA-3′) as oligonucleotide primers. The G7731A mutation creates a restriction site for *Dra*I and generates 96- and 34-bp fragments on *Dra*I digestion of PCR products. The restriction fragments were separated by electrophoresis in a 3% agarose gel. For quantification of G7731A mtDNA, I used ImageJ (Rasband WS, Image J, US National Institutes of Health, Bethesda, Maryland, USA, http://imagej.nih.gov/ij/, 1997–2014) software.

***Isolation of B82mt7731 cybrids***

I used mtDNA-less ($\rho^0$) B82 cells as recipients for G7731A mtDNA. $\rho^0$ B82 cells are resistant to BrdU and sensitive to hypoxanthine–aminopterin–thymidine (HAT) due to their deficiency of thymidine kinase activity. Furthermore, $\rho^0$ B82 cells are unable to grow in the absence of uridine and pyruvate due to their absence of mtDNA. mtDNA donor P29-69-183 cells were pretreated with cytochalasin B (10 μg/ml) for 10 min and centrifuged at 7,500 × *g* for 10 min at 37 °C for enucleation; the resultant cytoplasts were fused with $\rho^0$ B82 cells by using polyethylene glycol. The fusion mixture was cultured in selection medium containing 5-bromodeoxyuridine (BrdU; 30 μg/ml) and lacking uridine and pyruvate. The selection medium excluded unenucleated P29-69-183 cells and unfused $\rho^0$ B82 cells and thus allowed exclusive growth of *trans*-mitochondrial B82mt7731 cybrids.

***Isolation of ESmt7731 cybrids***

Host ES cells were pretreated with rhodamine 6G (R6G; 0.38–1.5 μg/ml in 3% ethanol) for 48 h to eliminate endogenous mitochondria and mtDNA (10, 11). The ES cells then were washed with PBS and suspended in R6G-free medium for 2 h to allow recovery. mtDNA donor B82mt7731 cybrids were pretreated with cytochalasin B (10 μg/ml) for 10 min and centrifuged at 22,500 × *g* for 30 min at 37 °C for enucleation. The resultant cytoplasts were fused with R6G-pretreated ES cells by using polyethylene glycol, and the fusion mixture was cultured in selection medium containing HAT to exclude unenucleated B82mt7731 cybrids. At 7 days after fusion, growing colonies were harvested for mtDNA genotyping. Under these selection conditions, ES cells containing

recovered endogenous mtDNA were not eliminated completely, owing to insufficient R6G treatment.

### *Generation of chimeric mice and mito-mice-tRNA$^{Lys7731}$*

Frozen 8-cell-stage embryos of ICR mice (ARK Resource Company) were thawed, and their zona pellucidae were removed by treatment with acidified Tyrode's buffer (Sigma–Aldrich). Each treated embryo was placed with about 50 ESmt7731 cybrids in a well of a 35-mm culture dish and incubated overnight to enable aggregation. The next day, the embryos were transferred into pseudopregnant ICR female mice (Japan SLC). The resulting progeny were identified by their coat-color chimerism. Founder ($F_0$) chimeric female mice were mated with C57BL/6 J (B6; CLEA Japan) male mice to produce the $F_1$ generation, and $F_1$ female mice with G7731A mtDNA in their tails ($F_1$ female mito-mice-tRNA$^{Lys7731}$) were backcrossed with B6 male mice to obtain $F_2$ mito-mice-tRNA$^{Lys7731}$.

### *Mice*

Inbred B6 mice generated through more than 40 rounds of brother–sister mating were obtained from CLEA Japan. I maintained mito-mice-tRNA$^{Lys7731}$ by repeated backcrossing of these female mice with B6 male mice. Animal experiments were performed in accordance with protocols approved by the Experimental Animal Committee of the University of Tsukuba, Japan.

### *Oxygen consumption*

Cells were washed once in PBS and then resuspended in PBS at a density of $4 \times 10^6$ cells/ml. Oxygen consumption was measured by using an oxygraph equipped with a Clark-type electrode (model 5300, Yellow Springs Instruments Company) at 37 °C. The cell suspension (2 ml) was transferred to a polarographic cell, and basal respiration was measured immediately under constant stirring.

### *Measurement of reactive oxygen species in mitochondria*

Reactive oxygen species were detected by using the mitochondrial superoxide indicator MitoSOX-Red (Invitrogen). Cells were incubated with 1 µM MitoSOX-Red for 15 min at 37 °C in PBS, washed twice with PBS, and then immediately analyzed by using flow cytometry (FACScan, Becton Dickinson).

### *Histopathologic analyses*

Formalin-fixed, paraffin-embedded sections (thickness, 5 µm) were stained with hematoxylin and eosin (H&E) to identify features characteristic of renal failures. Cryosections (thickness, 10 µm) of skeletal muscle were stained with modified Gomori trichrome for histopathologic analysis to identify RRFs. Cryosections (thickness, 10 µm) of renal tissues were prepared, and histologic analyses of cytochrome *c* oxidase (COX) and succinate dehydrogenase (SDH) activities were performed as described previously (12).

### *Grip strength test*

Muscle strength was estimated by using a Grip Strength Meter (Columbus Instruments); three sequential trials were performed on each mouse.

### *Biochemical measurements of respiratory enzyme activity*

Mitochondrial respiratory complex I (NADH dehydrogenase), complex II (succinate dehydrogenase), and complex III (cytochrome *c* reductase) are components of the electron-transport chain and are located in the mitochondrial inner membrane. The activity of these enzymes was assayed as described previously (13). Briefly, to estimate the activity due to complex I + III, NADH and cytochrome *c* (oxidized form) were used as substrates, and the reduction in cytochrome *c* was monitored by measuring absorbance at a wavelength of 550 nm. To estimate the activity due to complex II + III, sodium succinate and cytochrome *c* (oxidized form) were used as substrates, and the reduction of cytochrome *c* was monitored as described previously.

### *Measurement of blood glucose, lactate, and blood urea nitrogen (BUN)*

To determine fasting blood lactate and glucose concentrations, peripheral blood was collected from the tail veins of mice after overnight fasting from food. After oral administration of glucose (1.5 g/kg body weight), blood was collected again, and lactate and glucose concentrations were measured by using an automatic blood lactate test meter (Lactate Pro; Arkray) and glucose test meter (Dexter ZII; Bayer), respectively. BUN was measured by using a Urea N B test (Wako Pure Chemical, Osaka, Japan) in accordance with the manufacturer's protocol.

### *Measurement of hematocrit*

To determine hematocrit, capillary blood samples were obtained from each mouse by using heparinized capillary tubes, which then were centrifuged at 10,500 × *g* for 5 min. Packed cell volumes were measured by using a hematocrit reader.

### *Sequence analysis*

Each DNA (3 μg) extracted from P29-69-183 cells and from kidney of mito-mouse-tRNA$^{Lys7731}$ were used to prepare the sequencing libraries. These sequencing libraries were constructed by using the TruSeq DNA LT Sample Prep Kit (Illumina) according to the instructions in TruSeq DNA Sample Preparation Guide Rev. C (Illumina). These DNA samples were sheared by using an acoustic solubilizer (Covaris), and the overhangs resulting from the fragmentation were converted to blunt ends by phosphorylation of the DNA fragments. The blunt fragments were adenylated at their 3' ends were ligated to the ends of the DNA fragments, which were subsequently enriched by PCR. Clonal template clusters were generated from the sequencing library, and sequencing was performed by the reversible terminator-based method (14). Base calling and data conversion into Fastq files were performed by using software providing the Burrows-Wheeler Alignment Tool (15).

### *Statistical analysis*

Data are presented as mean ± SD and were analysed by using Student's t test or Tukey honestly significant difference test; *P* values less than 0.05 were considered significant. Excel (Microsoft) software was used for Student's t test and ANOVA, and R (The R

Foundation for Statistical Computing, http://www.R-project.org.)(16) was used for Tukey honestly significant difference test.

# RESULTS

***Cloning and sequence analysis of PCR products including tRNA genes***

To detect small proportion of mtDNA with somatic and possibly pathogenic mutations in the $tRNA^{Leu(UUR)}$ and $tRNA^{Lys}$ genes, I used two sets of primers so that the resulting PCR products would include the $tRNA^{Leu(UUR)}$ or $tRNA^{Lys}$ gene of P29 cells (Fig. 1). After cloning the PCR products, I sequenced all 43 clones obtained and compared the resulting sequences with that of mtDNA from P29 cells (Table 1). I found one and two somatic mutations in the mitochondrial $tRNA^{Leu(UUR)}$ and $tRNA^{Lys}$ genes, respectively. Given that each somatic mutation was present in only one of the 43 clones, the proportion of each in the mtDNA population of P29 cells would be about 2.2%.

The T7728C and G7731A mutations in the $tRNA^{Lys}$ gene both occurred in conserved sites (Table 2) and may correspond to pathogenic mutations that induce respiration defects by their accumulation. Moreover, an orthologous mutation to mouse G7731A has been reported to occur in human mtDNA from patients with mitochondrial diseases (17, 18).

Therefore, I selected these mutations in mtDNA for the generation of mito-mice. In an attempt to detect the T7728C and G7731A mutations in P29 mtDNA, I performed *Xmn*I and *Dra*I digestions of the PCR products of mtDNA, because the T7728C and G7731A mutations create an *Xmn*I site and a *Dra*I site, respectively (see MATERIALS & METHODS). However, the T7728C and G7731A mutations were undetectable due to their insufficient amounts in P29 cells.

### *Concentration of G7731A mtDNA in subclones of P29 cells*

Previous study showed that two mtDNA haplotypes with different mutations in single cells segregate stochastically during cell division (19). Therefore, some individual cells in the P29 population may possess detectable amounts of the mutated mtDNA. To obtain some individual cells that had accumulated either T7728C mtDNA or G7731A mtDNA from the P29 cell population, I isolated 100 subclones from P29 cells. Their mtDNA genotyping showed that two subclones, P29-42 and P29-69, possessed 34% and 48% G7731A mtDNA, respectively. However, I did not obtain any subclones carrying detectable amounts of T7728C mtDNA.

In the case of human mitochondrial tRNA gene mutations found in patients with mitochondrial diseases, respiration defects were apparent only when the mutated mtDNA had accumulated to more than 90% (20). To isolate P29 cells with more than 90% G7731A mtDNA, I cultured subclone P29-69, which had 48% G7731A mtDNA, for additional 3 months to allow further amplification of G7731A mtDNA through stochastic segregation; I then isolated more than 200 subclones from the P29-69 cells. I obtained one subclone, P29-69-183, which contained 92% G7731A mtDNA (Fig. 2A)—a level likely to be sufficient for the expression of respiration defects, if the G7731A mutation indeed is a pathogenic mutation.

### *Determination of the pathogenicity of G7731A mtDNA*

Comparison of the $O_2$ consumption rates between parental P29 cells and the P29-69-183 cells revealed the expression of respiration defects in the P29-69-183 cells (Fig. 2B). Moreover, P29-69-183 cells demonstrated slight overproduction of reactive

oxygen species (Fig. 2C), indicating the pathogenicity of the G7731A mutation. Whole-sequence analysis of mtDNA in P29-69-183 cells showed that the G7731A mutation is the only mutation in those cells that is capable of inducing respiration defects (Table 3). However, I had to resolve two important issues before generation of the mito-mice carrying G7731A mtDNA.

First, I had to confirm that the respiration defects in P29-69-183 cells were due to G7731A mtDNA and not to the selection of cells with mutations in nuclear DNA that were acquired during repeated recloning. Second, P29-69-183 cells could not be used as mtDNA donors to isolate mouse ES cells with G7731A mtDNA because of the difficulty of excluding unenucleated P29-69-183 cells from fusion mixtures of ES and enucleated P29-69-183 cells.

To simultaneously resolve these issues, I cytoplasmically transferred G7731A mtDNA from P29-69-183 cells into mtDNA-less ($\rho^0$) B82 cells (6). B82 cells are mouse fibrosarcoma cells that are resistant to 5-bromodeoxyuridine (BrdU) and sensitive to hypoxanthine–aminopterin–thymidine (HAT) due to their deficiency of thymidine kinase activity (6). Moreover, $\rho^0$ B82 cells are unable to grow in the absence of uridine and pyruvate due to their complete lack of mtDNA. Using selection medium containing BrdU and lacking uridine and pyruvate, I isolated two colonies, B82mt7731-1 and -2. Genotyping of mtDNA showed that B82mt7731-1 and -2 possessed 70% and 95% G7731A mtDNA, respectively (Fig. 3A), indicating the transfer of G7731A mtDNA from P29-69-183 cells into $\rho^0$ B82 cells.

I then examined the respiratory function of these 2 cybrids by estimating $O_2$ consumption rates and the amounts of reactive oxygen species. The B82mt7731-2

cybrids showed decreased $O_2$ consumption rates (Fig. 3B) and increased production of reactive oxygen species (Fig. 3C) compared with those of B82mtB6 cybrids containing normal mtDNA from B6 mice. Therefore, respiration defects were transferred to B82mt7731 cybrids concurrently with the transfer of G7731A mtDNA from P29-69-183 cells into $\rho^0$ B82 cells, suggesting that the somatic G7731A mutation in mtDNA is a pathogenic mutation that can induce mitochondrial respiration defects by its predominant accumulation. Furthermore, B82mt7731 cybrids are effective as donors of G7731A mtDNA to ES cells, because unenucleated B82mt7731 cybrids can be excluded by using selection medium containing HAT.

***Isolation of ES cells containing G7731A mtDNA and their chimeric mice***

Previous study showed that no chimeric mice were obtained from ES cells carrying predominant amounts of ΔmtDNA, because the significant respiration defects induced by ΔmtDNA inhibited differentiation of ES cells to various tissues and germ cells (21). Therefore, I was concerned that the transfer of mtDNA from B82mt7731-2 cybrids containing 95% G7731A mtDNA to ES cells would inhibit generation of chimeric mice, and instead used B82mt7731-1 cybrids containing lower proportions of G7731A mtDNA (Fig. 3A) as mtDNA donors.

Female (XO)-type ES cells (TT2 cells) were pretreated with rhodamine 6G (R6G) to eliminate endogenous mitochondria and mtDNA. They then were used as recipients of G7731A mtDNA and fused with enucleated B82mt7731-1 cybrids. The fusion mixture was cultured in selection medium containing HAT to exclude unenucleated B82mt7731-1 cybrids. Seven ES clones grew in the selective medium, two of which—clones ESmt7731-4 and -7—contained G7731A mtDNA (Fig. 4). The

absence of G7731A mtDNA in the remaining five clones may be due to incomplete elimination of endogenous mtDNA in ES cells during R6G pretreatment.

I then aggregated the ESmt7731-4 and -7 cybrid clones with 8-cell-stage mouse embryos (ICR strain) and obtained 35 $F_0$ chimeric mice. Because mouse mtDNA is inherited strictly maternally (22, 23), I selected 15 $F_0$ chimeric female mice with 13%–76% G13997A mtDNA in their tails as founder mice (Table 4) and mated them with B6 male mice to generate $F_1$ mice that carried G7731A mtDNA due to its transfer through the female germline.

***Generation of mito-mice-tRNA$^{Lys7731}$ via female germ line transfer of G7731A mtDNA***

Of the 15 $F_0$ female chimeras, 11 produced a total of 121 $F_1$ pups, 63 of which had G7731A mtDNA in their tails (Table 4). This finding suggests that G7731A mtDNA was transmitted maternally from $F_0$ female mice to $F_1$ progeny. Mice that carried G7731A mtDNA derived from lung carcinoma P29 cells were named 'mito-mice-tRNA$^{Lys7731}$'.

Of the 63 $F_1$ mice with G7731A mtDNA in their tails, seven $F_1$ female mice carrying high proportions of G7731A mtDNA were mated with B6 male mice to obtain subsequent generations ($F_2$-$F_5$) of mito-mice-tRNA$^{Lys7731}$ with sufficient G7731A mtDNA for the expression of respiration defects and resultant disorders. The proportions of G7731A mtDNA varied significantly among the pups born to each dam, but none of the pups carried more than 85% G7731A mtDNA (Fig. 5A).

To examine the reasons for the lack of mito-mice-tRNA$^{Lys7731}$ with more than 85% G7731A mtDNA, I estimated the proportion of G7731A mtDNA in the oocytes

obtained by ovarian hyperstimulation of $F_5$ female mito-mice-tRNA$^{Lys7731}$ with high proportions of G7731A mtDNA. The results again showed significant variation in G7731A mtDNA proportions among the oocytes and the absence of the oocytes with more than 85% G7731A mtDNA (Fig. 5B), indicating that lethality of oocytes with high levels of G7731A mtDNA is responsible for the absence of mito-mice-tRNA$^{Lys7731}$ carrying more than 85% G7731A mtDNA.

My observations suggest that mito-mice-tRNA$^{Lys7731}$ at least in part can serve as models to investigate pathogenesis of mitochondrial diseases that arise due to mutations in the mitochondrial tRNA genes. In addition, the transmission profiles of G7731A mtDNA showed that selecting oocytes with lower levels of the mutated mtDNA likely would be effective to prevent maternal transmission of the disease phenotypes to the progeny.

***Expression of disorders in mito-mice-tRNA$^{Lys7731}$ with predominant G7731A mtDNA***

I used B6 mice as controls and three groups of $F_5$ young (4-months-old) mito-mice-tRNA$^{Lys7731}$ with different heteroplasmic conditions (low, intermediate, and high levels of G7731A mtDNA) in their tails to examine various phenotypes relevant to mitochondrial diseases (Fig. 6).

First, I analyzed body length (Fig. 6A) and muscle strength (Fig. 6B), because abnormalities in these characteristics frequently occur in patients with mitochondrial diseases (17, 18), and these parameters can be examined without euthanizing the young mice. Unlike mito-mice-tRNA$^{Lys7731}$ with low and intermediate levels, those with high levels of G7731A mtDNA showed short body length (Fig. 6A) and muscle weakness

(Fig. 6B), which are closely associated with the clinical phenotypes caused by mutations in the mitochondrial *tRNA*$^{Lys}$ gene (2, 17, 18).

I then quantitatively estimated mitochondrial respiratory function and revealed respiration defects in skeletal muscle and kidney from mito-mice-tRNA$^{Lys7731}$ with high levels of G7731A mtDNA (Fig. 6C). Therefore, accumulation of G7731A mtDNA likely is responsible for the respiration defects in mito-mice-tRNA$^{Lys7731}$ with high levels of G7731A mtDNA (Fig. 6C). These respiration defects in the skeletal muscle subsequently result in the expression of muscle weakness (Fig. 6B), which corresponds to a phenotype relevant to mitochondrial diseases (2).

In contrast, other metabolic parameters relevant to mitochondrial diseases were normal in young mito-mice-tRNA$^{Lys7731}$ (Fig. 7). Histochemical analysis showed that ragged-red fibers (RRF) frequently observed in MERRF patients (2) and renal failures frequently observed in mito-mice-Δ (4, 5) were not found in young mito-mice-tRNA$^{Lys7731}$ (Figs. 8 and 9). Absence of these disorders in mito-mice-tRNA$^{Lys7731}$ may be due in part to that G7731A mtDNA proportions in them were not sufficient to induce significant respiration defects. For example, G8344A mtDNA proportions exceed 85% in patients with MERRF (2). My failure to obtain mito-mice-tRNA$^{Lys7731}$ with more than 85% G7731A mtDNA can be explained by the lethality of mouse oocytes carrying these levels of G7731A mtDNA (Fig. 5B).

***Late-onset metabolic abnormalities in aged mito-mice-tRNA$^{Lys7731}$***

I then used aged (26-month-old) male mito-mice-tRNA$^{Lys7731}$ with low (< 5%) or high (70% to 75%) levels of G7731A mtDNA in their tails at 4 weeks after birth and

age- and sex-matched B6 mice (negative controls). First, I evaluated body length (Fig. 10A) and muscle strength (Fig. 10B), because abnormalities in these phenotypes are expressed in young (4-month-old) mito-mice-tRNA$^{Lys7731}$ (Fig. 6A and B) and can be examined without killing the mice. Short body length (Fig. 10A) and muscle weakness (Fig. 10B), which are closely associated with the clinical abnormalities caused by the orthologous G8328A mutation in the human mitochondrial *tRNA*$^{Lys}$ gene (17, 18), occurred exclusively in young mito-mice-tRNA$^{Lys7731}$ with high levels of G7731A mtDNA

I then examined various metabolic parameters relevant to mitochondrial diseases. Whereas these features were normal in young mito-mice-tRNA$^{Lys7731}$ (Fig. 7), I expected that abnormalities in these parameters would be expressed as late-onset disorders as the mito-mice-tRNA$^{Lys7731}$ aged. Unlike aged B6 mice and aged mito-mice-tRNA$^{Lys7731}$ with low levels of G7731A mtDNA, aged mito-mice-tRNA$^{Lys7731}$ with high levels of G7731A mtDNA exclusively had low hematocrit values (Fig. 10C), lactic acidosis (Fig. 10D), and increased levels of BUN in the peripheral blood (Fig. 10E). In contrast, although patients with mitochondrial diseases sometimes demonstrate mitochondrial diabetes (1–3), neither group of aged mito-mice-tRNA$^{Lys7731}$ manifested hyperglycemia (Fig. 10F). Therefore, except for hyperglycemia, the metabolic abnormalities seen in patients with mitochondrial diseases were expressed as late-onset disorders in aged mito-mice-tRNA$^{Lys7731}$ with high levels of G7731A mtDNA.

***Lifespan and tissue abnormalities in euthanized moribund mito-mice-tRNA$^{Lys7731}$***

I then assessed the lifespans of mito-mice-tRNA$^{Lys7731}$ and the tissue abnormalities in euthanized moribund mice. The median survival times in B6 mice and in mito-mice-tRNA$^{Lys7731}$ with low or high levels of G7731A mtDNA were 26, 28, and 27 months, respectively (Fig. 11). Thus, median survival times did not differ significantly between mito-mice-tRNA$^{Lys7731}$ with high and low levels of G7731A mtDNA.

Gross necropsy of euthanized moribund mice showed that muscle atrophy (Fig. 12A) and anemic kidneys (Fig. 13A) occurred exclusively in mito-mice-tRNA$^{Lys7731}$ with high levels of G7731A mtDNA. Muscle atrophy occurs not only in elderly men and women (45) and patients with mitochondrial diseases (46) but also in mtDNA mutator mice (47, 48) and mito-mice-Δ that express significant respiration defects (49). Moreover, renal abnormalities have been reported to occur occasionally in patients with mitochondrial diseases (50–52) and in mito-mice-Δ that express significant respiration defects (4, 5).

I then histologically analyzed these tissues to characterize the macroscopic abnormalities in greater detail. First, I used modified Gomori trichrome staining to reveal RRFs that occur frequently in patients with mitochondrial diseases (2). However, even aged mito-mice-tRNA$^{Lys7731}$ with high levels of G7731A mtDNA lacked RRFs in skeletal muscle (Fig. 12B); this was consistent with recent findings in mtDNA mutator mice and mito-mice-Δ (49).

Although the skeletal muscle was histologically normal, the anemic kidneys demonstrated multiple abnormalities. The renal cortical tubules of aged mito-mice-tRNA$^{Lys7731}$ with high levels of G7731A mtDNA were dilated and contained casts; these changes, indicative of renal failures, did not occur in aged B6 mice or in aged mito-mice-tRNA$^{Lys7731}$ with low levels of mutated mtDNA (Fig. 13B). Given that young mito-mice-tRNA$^{Lys7731}$ lacked similar renal changes (Fig. 9), these changes correspond to a late-onset disorder. Histologic analysis of mitochondrial respiratory function revealed decreased mitochondrial COX activity in the kidney tissue of aged mito-mice-tRNA$^{Lys7731}$ with high levels of G7731A mtDNA (Fig. 13C). Therefore, the respiration defects in mito-mice-tRNA$^{Lys7731}$ with high levels of G7731A mtDNA (Fig. 13C) likely caused their renal failures (Fig. 13B).

***Genotyping of G7731A mtDNA in tissues of mito-mice-tRNA$^{Lys7731}$***

For the purposes of this study, I classified 4-week-old mito-mice-tRNA$^{Lys7731}$ as having low or high amounts of mutated mtDNA by estimating the proportions of G7731A mtDNA isolated from samples of tail tissue. The question that then arises is whether the proportions of G7731A mtDNA differ among tissues or with age.

# DISCUSSION

The current study generated mito-mice-tRNA$^{Lys7731}$ carrying G7731A mtDNA with a pathogenic G7731A mutation in the mitochondrial *tRNA*$^{Lys}$ gene. Specifically, I concentrated a small proportion of mtDNA with a somatic G7731A mutation that was present in P29 cells and then introduced it into ES cells to generate mito-mice-tRNA$^{Lys7731}$. The resulting mice were used to investigate the pathogenesis and transmission profiles of G7731A mtDNA.

Regarding the pathogenesis of G7731A mtDNA, young mito-mice-tRNA$^{Lys7731}$ with 74%-84% G7731A mtDNA demonstrated respiration defects and the resultant muscle weakness and short body length (Fig. 6). These abnormalities in these mice are very similar to those found in patients with mitochondrial diseases due to human orthologous G8328A mutation (17, 18) and in MERRF patients carrying the G8344A mutation in the *tRNA*$^{Lys}$ gene (2, 24–26). Although these abnormalities were expressed in mito-mice-tRNA$^{Lys7731}$ with 74%-84% G7731A mtDNA (Fig. 6) and in the patients with 57% (17) and 82% G8328A mtDNA (18), more than 85% G8344A mtDNA was required for the onset of severe abnormalities in patients with MERRF (2, 24–26). However, I could not obtain mito-mice-tRNA$^{Lys7731}$ with more than 85% G7731A mtDNA (Fig. 5A), which would be expected to induce significant respiration defects and severe abnormalities corresponding to MERRF, owing to the lethality of mouse oocytes with more than 85% G7731A mtDNA (Fig. 5B). Therefore, the expression of the significant respiration defects and severe clinical disorders in MERRF patients can be explained by supposing the absence of lethality in human oocytes even at G8344A mtDNA levels exceeding 85%. In contrast, previous studies (4, 5) showed that mito-mice-Δ possessed more than 85% ΔmtDNA with a large-scale deletion, and expressed significant respiration defects and severe abnormalities, even though their

oocytes did not have more than 80% ΔmtDNA (27). The increase in the proportion of ΔmtDNA after birth may be due to its replication advantage (4, 5).

The absence of abnormalities in mito-mice-tRNA$^{Lys7731}$ with intermediate levels (37%-56%) of G7731A mtDNA (Fig. 6A and B) appears to be different from what is observed for mtDNA with human orthologous G8328A mutation, because the patient with only 57% G8328A mtDNA in the skeletal muscles expressed disorders (17). This apparent discrepancy may be due to the aging effects in the patient with 57% G8328A mtDNA, considering that the phenotypes of the mito-mice-tRNA$^{Lys7731}$ were examined 4 months after the birth (Fig. 6), and that the patient expressed disorders 45 years after the birth (17). Thus, I have to examine whether mito-mice-tRNA$^{Lys7731}$ with intermediate levels of G7731A mtDNA express abnormalities along with their aging.

Regarding transmission profiles, those of mito-mice-tRNA$^{Lys7731}$ are highly similar to those of MERRF patients, in that the mutated mtDNA is inherited to subsequent generations through the female germline, and the proportion of mutated mtDNA varied markedly among the pups born to each dam (Fig. 5A). The pups always carry wild-type mtDNA (Fig. 5A), due to the significant pathogenicity of G7731A mtDNA and resultant induction of oocyte lethality in the absence of wild-type mtDNA (Fig. 5B). In contrast, previously generated mito-mice-COI$^{6589}$ (6) and mito-mice-ND6$^{13997}$ (7, 8), which carry a 100% (homoplasmic) T6589C mtDNA mutation and a homoplasmic G13997A mtDNA mutation in the structural genes *COXI* and *ND6*, respectively, due to the mild pathogenicity of the mutations. Because patients with MERRF and mito-mice-tRNA$^{Lys7731}$ always carry both wild-type mtDNA and

mutated mtDNA, mito-mice-tRNA$^{Lys7731}$ are appropriate models for further investigating the transmission profiles of mutated mtDNA with marked pathogenicity.

The heteroplasmic mtDNA (wild-type mtDNA and mutated G7731A mtDNA) of these mito-mice-tRNA$^{Lys7731}$ segregated stochastically, like those derived from different mouse strains (BALB and NZB) with polymorphic mutations (28) and those with and without point mutations (29). The significant variation in the G7731A mtDNA proportions among pups (Fig. 5A) may reflect 'bottleneck effects' with (30, 31) or without decrease in the mtDNA copy number (32, 33) during female germline transmission of the heteroplasmic mtDNAs.

Regarding primary prevention of mitochondrial diseases, the results in Figs. 5 and 6 indicate that the selection of oocytes with low proportions of G7731A mtDNA likely would yield phenotypically normal mice. In contrast, previous study (27) showed that nuclear transplantation from zygotes of *trans*-mitochondrial mito-mice-Δ into enucleated zygotes with normal mtDNA is effective as germline gene therapy. Many recent reports similarly have noted that the use of the nuclear transplantation from human oocytes of affected mothers into enucleated oocytes donated by unrelated women would prevent the transmission of mitochondrial diseases caused by mtDNA mutations to their children (34–36). However, this technology includes the risk of inducing nuclear abnormalities, even though it excludes the risk of mitochondrial abnormalities. This problem would be resolved by the selection of oocytes with low proportions of mutated mtDNA. Previous study showed that polar bodies are effective for preimplantation genetic diagnosis (PGD) to deduce the proportion of mutated mtDNA in mouse oocytes (27). However, subsequent studies using polar bodies from

human oocytes (37) and blastomeres from human embryos (38, 39) indicated that blastomeres are more appropriate than the polar bodies for PGD to deduce the proportion of mutated mtDNA. Although this procedure would not completely exclude the mutated mtDNA from the affected mothers, previous studies (40, 41) showed the presence of inter-mitochondrial complementation to maintain normal respiratory function in the presence of the mutated mtDNA. Therefore, in light of the results in Figs. 5 and 6, I propose that the selection of embryos with low proportions of mutated mtDNA from affected mothers by diagnosing the blastomeres would be effective for obtaining unaffected children.

Using mito-mice-tRNA$^{Lys7731}$, I showed that high levels of G7731A mtDNA and the resultant respiration defects did not affect median survival times (Fig. 11), even though they induced the late-onset disorders (Figs. 10, 12 and 13). In contrast, accumulation of pathogenic mutations in human mtDNA and the resultant respiration defects have been proposed to be responsible for features of normal aging as well as of mitochondrial diseases (1–3). However, current observations suggest that mtDNA with pathogenic mutations is not necessarily associated with aging processes. This idea is further supported by previous findings that mito-mice-COI$^{6589}$, which contain mtDNA with a T6589C mutation in *COI*, and mito-mice-ND6$^{13997}$, which carry mtDNA with a G13997A mutation in *ND6*, had normal lifespans (8).

In contrast, these mito-mice-tRNA$^{Lys7731}$ developed several phenotypes relevant to mitochondrial diseases, including anemia (Fig. 10C), lactic acidosis (Fig. 10D), and increased BUN (Fig. 10E). Moreover, euthanized moribund mito-mice-tRNA$^{Lys7731}$ showed muscle atrophy (Fig. 13A) and renal failures (Fig. 13).

The muscle atrophy in aged mito-mice-tRNA$^{Lys7731}$ with high levels of G7731A mtDNA (Figs. 12A) likely is associated with their muscle weakness (Fig. 10B). It is also likely that the anemic kidney tissue in the aged mito-mice-tRNA$^{Lys7731}$ (Fig. 13A) reflects their low hematocrit levels (Fig. 10C). Moreover, the increased BUN values (Fig. 10E) likely reflect the renal failures (Fig. 13B) caused by high levels of G7731A mtDNA and the resultant respiration defects (Fig. 13C). Given that mito-mice-tRNA$^{Lys7731}$ with low and high levels of G7731A mtDNA have the same B6 nuclear genetic background, the respiration defects induced exclusively by the high levels of G7731A mtDNA are responsible for the development of these late-onset disorders.

A question that then arises is why these abnormalities have a late onset in mito-mice-tRNA$^{Lys7731}$. One explanation is the requirement of long-term exposure of the tissues to respiration defects or the requirement of age-dependent development of nuclear abnormalities for the onset of these disorders. It is also likely that each cell in a tissue eventually contains solely mtDNA either with or without the G7731A mutation as a consequence of stochastic segregation over time (19, 28 29), resulting in the induction of the late-onset disorders due to the apoptosis or substantial dysfunction of cells containing only G7731A mtDNA.

In contrast to their other clinically characteristic features, aged mito-mice-tRNA$^{Lys7731}$ with high levels of G7731A mtDNA did not demonstrate peripheral hyperglycemia (Fig. 10F) indicative of mitochondrial diabetes; this disorder has been proposed to occur frequently in patients with mitochondrial diseases (1–3). However, these results are consistent with previous findings in mito-mice-COI$^{6589}$, which have normal blood glucose levels (6). In addition, blood glucose levels were low

in mito-mice-Δ (53) but high in mito-mice-ND6$^{13997}$ (8), indicating that high levels of pathogenic mtDNA mutations and the resultant respiration defects do not necessarily cause mitochondrial diabetes.

Current study also showed that all groups of these mice—even aged mito-mice-tRNA$^{Lys7731}$ with high levels of G7731A mtDNA (that is, 70% to 75%)—lacked RRFs (Fig. 12B). The absence of RRFs may be due in part to the fact that the amount of G7731A mtDNA was insufficient to induce RRFs. Thus, somehow mito-mice-tRNA$^{Lys7731}$ with more than 75% G7731A mtDNA have to be generated for RRF development. However, the death of B6 mouse oocytes that carry levels of G7731A mtDNA in excess of 85% (Fig. 5) would prevent the generation of mito-mice-tRNA$^{Lys7731}$ with sufficient proportions of G7731A mtDNA to develop RRFs. It is likely that some as-yet unknown nuclear factors in mouse strains other than B6 may allow the survival of oocytes with more than 85% G7731A mtDNA.

To evaluate this idea, I plan to replace the B6 nuclear genetic background of mito-mice-tRNA$^{Lys7731}$ with that from other strains. This replacement may support the survival of oocytes with more than 85% G7731A mtDNA and subsequently the development of skeletal muscle RRFs and peripheral hyperglycemia in the resultant mito-mice-tRNA$^{Lys7731}$.

# ACKNOWLEDGEMENTS

I am grateful to Dr. Keizo Takenaga at Shimane University, and Professor Satoru Takahashi at University of Tsukuba for their helpful advice and kind cooperation.

I am most grateful to Professor Kazuto Nakada, Professor Jun-Ichi Hayashi and Assistant Professor Kaori Ishikawa at University of Tsukuba, for their continuous guidance and valuable discussion through my doctoral program.

Finally, I thank all of my colleagues of Professor Nakada's laboratory for their support in this study and my family for their support of my life in University of Tsukuba.

# REFERENCES

1. Larsson N-G, Clayton DA (1995) Molecular genetic aspects of human mitochondrial disorders. *Annu Rev Genetics* 29:151-178.
2. Wallace DC (1999) Mitochondrial diseases in man and mouse. *Science* 283(5407):1482-1488.
3. Taylor RW, Turnbull DM (2005) Mitochondrial DNA mutations in human disease. *Nat Rev Genet* 6(5):389-402.
4. Inoue K, et al. (2000) Generation of mice with mitochondrial dysfunction by introducing mouse mtDNA carrying a deletion into zygotes. *Nat Genet* 26(2):176-181.
5. Nakada K, et al. (2001) Inter-mitochondrial complementation: Mitochondria-specific system preventing mice from expression of disease phenotypes by mutant mtDNA. *Nat Med* 7(8):934-940.
6. Kasahara A, et al. (2006) Generation of *trans*-mitochondrial mice carrying homoplasmic mtDNAs with a missense mutation in a structural gene using ES cells. *Hum Mol Genet* 15(6):871-881.
7. Yokota M, et al. (2010) Generation of *trans*-mitochondrial mice carrying homoplasmic mtDNAs with a missense mutation in a structural gene using ES cells. *FEBS Lett* 584(18):3943-3948.
8. Hashizume O, et al. (2012) Specific mitochondrial DNA mutation in mice regulate diabetes and lymphoma development. *Proc Natl Acad Sci USA* 109(26):10528-1053.
9. Ishikawa K, et al. (2008) ROS-generating mitochondrial DNA mutations can regulate tumor cell metastasis. *Science* 320(5876):661-664.

10. Ziegler ML, Davidson RL (1981) Elimination of mitochondrial elements and improved viability in hybrid cells. *Somatic Cell Genet* 7(1):73–88.
11. McKenzie M, Trounce IA, Cassar CA, Pinkeert CA (2004) Production of homoplasmic xenomitochondrial mice. *Proc Natl Acad Sci USA* 101(6):1685–1690.
12. Wang J, et al. (1999) Dilated cardiomyopathy and atrioventricular conduction blocks induced by heart-specific inactivation of mitochondrial DNA gene expression. *Nat Genet* 21(1):133-137.
13. Miyabayashi S, et al. (1989) Defective pattern of mitochondrial respiratory enzymes in mitochondrial myopathy. *J Inher Metab Dis* 12(3):373–377.
14. Bentley DR, et al. (2008) Accurate whole human genome sequencing using reversible terminator chemistry. *Nature* 456(7218):53-59.
15. Li H, Durbin R (2009) Fast and accurate short read alignment with Burrows–Wheeler Transform. *Bioinformatics* 25(14):1754-1760.
16. Ihaka R, Gentleman R (1996) R: a language for data analysis and graphics. *J Comp Graph Stat* 5(3):299-314.
17. Houshmand M, Lindberg C, Moslemi AR, Oldfors A, Holme E (1999) A novel heteroplasmic point mutation in the mitochondrial tRNA(Lys) gene in a sporadic case of mitochondrial encephalomyopathy: de novo mutation and no transmission to the offspring. *Hum Mutat* 13(3):203-209.
18. Blakely EL, et al. (2007) Sporadic myopathy and exercise intolerance associated with the mitochondrial 8328G>A tRNALys mutation. *J Neurol* 254(9):1283-1285.
19. Hayashi J-I, Tagashira Y, Yoshida MC, Ajiro K, Sekiguchi T (1983) Two distinct types of mitochondrial DNA segregation in mouse-rat hybrid cells: stochastic segregation and chromosome-dependent segregation. *Exp Cell Re*s 147(1):51-61.

20. Chomyn A, et al. (1992) MELAS mutation in mtDNA binding site for transcription termination factor causes defects in protein synthesis and in respiration but no change in levels of upstream and downstream mature transcripts. *Proc Natl Acad Sci USA* 89(10):4221-4225.
21. Ishikawa K, et al. (2005) Application of ES cells for generation of respiration-deficient mice carrying mtDNA with a large-scale deletion. *Biochem Biophys Res Commun* 333(2):590-595.
22. Kaneda H, et al. (1995) Elimination of paternal mitochondrial DNA in intraspecific crosses during early mouse embryogenesis. *Proc Natl Acad Sci USA* 92(10):4542-4546.
23. Shitara H, Hayashi J-I, Takahama S, Kaneda H, Yonekawa H (1998) Maternal inheritance of mouse mtDNA in interspecific hybrids: segregation of the leaked paternal mtDNA followed by the prevention of subsequent paternal leakage. *Genetics* 148(2):851-857.
24. Hammans SR, et al. (1993) The mitochondrial DNA transfer $RNA^{Lys}$ A → $G^{(8344)}$ mutation and the syndrome of myoclonic epilepsy with ragged red fibres (MERRF). *Brain* 116( Pt 3):617-632.
25. Hammans SR, et al. (1995) The mitochondrial DNA transfer $RNA^{Leu(UUR)}$ A → $G^{(3243)}$ mutation. A clinical and genetic study. *Brain* 118 ( Pt 3):721-734.
26. Chinnery P, Howell N, Lightowlers RN, Turnbull DM (1998) MELAS and MEFFR: The relationship between maternal mutation load and the frequency of clinically affected offspring. *Brain* 121( Pt 10):1889-1894.
27. Sato A, et al. (2005) Gene therapy for progeny of mito-mice carrying pathogenic mtDNA by nuclear transplantation. *Proc Natl Acad Sci USA* 102(46):16765-16770.

28. Jenuth JP, Peterson AC, Fu K, Shoubridge EA (1996) Random genetic drift in the female germline explains the rapid segregation of mammalian mitochondrial DNA. *Nat Genet* 14(2):146-151.
29. Freyer C, et al. (2012) Variation in germline mtDNA heteroplasmy is determined prenatally but modified during subsequent transmission. *Nat Genet* 44(11): 1282-1285.
30. Cree LM, et al. (2008) A reduction of mitochondrial DNA molecules during embryogenesis explains the rapid segregation of genotypes. *Nat Genet* 40(2):249-254.
31. Wai T, Teoli D, Shoubridge EA (2008) The mitochondrial DNA genetic bottleneck results from replication of a subpopulation of genomes. *Nat Genet* 40(12): 1484-1488.
32. Cao L, et al. (2007) The mitochondrial bottleneck occurs without reduction of mtDNA content in female mouse germ cells. *Nat Genet* 39(3):386-390.
33. Cao L, et al. (2009) New evidence confirms that the mitochondrial bottleneck is generated without reduction of mitochondrial DNA content in early primordial germ cells of mice. *PLoS Genet* 5(12): e1000756.
34. Craven L, et al. (2010) Pronuclear transfer in human embryos to prevent transmission of mitochondrial DNA diseases. *Nature* 465(7294):82-85.
35. Tachibana M, et al. (2013) Towards germline gene therapy of inherited mitochondrial diseases. *Nature* 493(7434):627-631.
36. Paull D, et al. (2013) Nuclear genome transfer in human oocytes eliminates mitochondrial DNA variants. *Nature* 493(7434):632-637.

37. Gigarel N, et al. (2011) Poor correlations in the levels of pathogenic mitochondrial DNA mutations in polar bodies versus oocytes and blastomeres in humans. *Am J Hum Genet* 88(4):494-498.

38. Steffann J, et al. (2006) Analysis of mtDNA variant segregation during early human embryonic development: a tool for successful NARP preimplantation diagnosis. *J Med Genet* 43(3):244-247.

39. Tajima H, et al. (2007) The development of novel quantification assay for mitochondrial DNA heteroplasmy aimed at preimplantation genetic diagnosis of Leigh encephalopathy. *J Assist Reprod Genet* 24(6):227-232.

40. Hayashi J-I, Takemitsu M, Goto Y-I, Nonaka I (1994) Human mitochondria and mitochondrial genome function as a single dynamic cellular unit. *J Cell Biol* 125(1):43-50.

41. Ono T, Isobe K, Nakada K, Hayashi J-I (2001) Human cells are protected from mitochondrial dysfunction by complementation of DNA products in fused mitochondria. *Nat Genet* 28(3):272-275.

42. Cohen BH. (1991) Introduction of disease-related mitochondrial DNA deletions into HeLa cells lacking mitochondrial DNA results in mitochondrial dysfunction. *Proc Natl Acad Sci U S A* 88(23):10614-10618.

43. Chomyn A, et al. (1991) In vitro genetic transfer of protein synthesis and respiration defects to mitochondrial DNA-less cells with myopathy-patient mitochondria. *Mol Cell Biol.* 11(4):2236-2244.

44. King MP, Koga Y, Davidson M, Schon EA (1992) Defects in mitochondrial protein synthesis and respiratory chain activity segregate with the $tRNA^{Leu(UUR)}$

mutation associated with mitochondrial myopathy, encephalopathy, lactic acidosis, and strokelike episodes. *Mol Cell Biol* 12(2):480-490.

45. Nedergaard A, Henriksen K, Karsdal MA, Christiansen C (2013) Musculoskeletal ageing and primary prevention. *Best Pract Res Clin Obstet Gynaecol* 27(5):673-688.

46. Cohen BH (2013) Neuromuscular and systemic presentations in adults: diagnoses beyond MERRF and MELAS. *Neurotherapeutics* 10 (2):227-242.

47. Trifunovic A, et al. (2004) Premature ageing in mice expressing defective mitochondrial DNA polymerase. *Nature* 429 (6990):417-423.

48. Kujoth GC, et al. (2005) Mitochondrial DNA mutations, oxidative stress, and apoptosis in mammalian aging. *Science* 309(5733):481-484.

49. Mito T, et al. (2015) Transmitochondrial mito-miceΔ and mtDNA mutator mice, but not aged mice, share the same spectrum of musculoskeletal disorders. *Biochem Biophys Res Commun* 456(4):933-937.

50. Rötig A, et al. (1992) Maternally inherited duplication of the mitochondrial genome in a syndrome of proximal tubulopathy, diabetes mellitus, and cerebellar ataxia. *Am J Hum Genet* 50(2):364-370.

51. Jansen JJ, et al. (1997) Mutation in mitochondrial $tRNA^{Leu(UUR)}$ gene associated with progressive kidney disease. *J Am Soc Nephrol* 8(7):1118-1124.

52. Szabolcs MJ, et al. (1994) Mitochondrial DNA deletion: a cause of chronic tubulointerstitial nephropathy. *Kidney Int* 45(5):1388-1396.

53. Nakada K, et al. (2004) Accumulation of pathogenic ΔmtDNA induced deafness but not diabetic phenotypes in mito-mice. *Biochem Biophys Res Commun* 323(1):175-184.

# TABLES

**Table 1**

**Somatic mutations in P29 mtDNA according to cloning and sequence analysis of the PCR products including the *tRNA*$^{Leu(UUR)}$ and *tRNA*$^{Lys}$ genes**

| No. of clones | tRNA genes | *Leu*$^{UUR}$ | *Ile* | *Met* | *Ser*$^{CUN}$ | *Lys* | *Lys* |
|---|---|---|---|---|---|---|---|
| | nucleotide position | 2721 | 3760 | 3883 | 6931 | 7728† | 7731‡ |
| | P29 sequence* | T | G | - | T | T | G |
| 1 | | del | - | - | - | - | - |
| 1 | | - | A | - | - | - | - |
| 1 | | - | - | insA | - | - | - |
| 1 | | - | - | - | C | - | - |
| 1 | | - | - | - | - | C | - |
| 1 | | - | - | - | - | - | A |
| 37 | | - | - | - | - | - | - |

* Registered under the GenBank accession number EU312160.

† The T7728C mutation in the *tRNA*$^{Lys}$ gene occurred in a site highly conserved throughout animals and fungi (see Table 3). The mutation affects the first base of an anticodon triplet (TTT), resulting in an anticodon swap from TTT to CTT (Lys to Glu).

‡ The mutation equivalent to the G7731A mutation in the *tRNA*$^{Lys}$ gene of mice has been reported to occur in the mtDNA from human patients with mitochondrial diseases (17, 18).

**Table 2**

**Comparison of mutations in the mouse mitochondrial tRNA gene with the wild-type tRNA genes of other species**

| | *Leu(UUR)* | *Lys* | |
|---|---|---|---|
| | del2721T | T7728C | G7731A |
| Mutation | — | C | A |
| Mouse | T | T | G |
| Human | C | T | G |
| *Xenopus* | T | T | G |
| Zebrafish | C | T | G |
| *Drosophila* | T | T | A |
| Nematoda | — | T | T |
| Yeast | C | T | G |

The GenBank accession numbers of the sequences used in the alignment are: mouse, AY172335; human, NC_012920; *Xenopus*, NC_001573; zebrafish, NC_002333; *Drosophila*, NC001709; Nematoda, NC_001328; yeast, NC_001224.

**Table 3**

**Whole-sequence analysis of the mtDNA from P29-69-183 cells**

| genes | *tRNA*$^{Lys}$ | *tRNA*$^{Arg}$ | | | D-loop | |
|---|---|---|---|---|---|---|
| nucleotide position | 7731 | 9818– | 9821– | | 16099 | 16105 |
| P29 sequence* | G | $(T)_3$ | $(A)_9$ | $(A)_9$ | A | T |
| variant sequence | A | $(T)_2$ | $(A)_8$ | $(A)_{10}$ | C | C |
| P29-69-183** | 89.6%† | 16.4% | 8.2% | 6.5% | 31.6% | 47.6% |
| mito-mouse-tRNA$^{Lys7731}$‡ | 80.0% | 3.6% | 0.5% | 18.1% | 26.9% | 37.0% |

* P29 mtDNA sequence, GenBank accession number EU312160.

**Registered under GenBank accession no. AP014540.

† Whole-sequence analysis of mtDNA from P29-69-183 cells showed that they had 89.6% G7731A mtDNA. This value was almost equivalent to that obtained in Fig. 2A (92%), suggesting the reliability of my quantification of G7731A mtDNA proportion by using restriction fragment length polymorphism.

‡Kidney of $F_5$ mito-mouse-tRNA$^{Lys7731}$ possessing 81.3% G7731A mtDNA quantified by using restriction fragment length polymorphism was used for whole-sequence analysis of the mtDNA. All polymorphic mutations found in mtDNA of P29-69-183 cells have persisted in mtDNA of a mito-mouse-tRNA $^{Lys7731}$. Registered under GenBank accession no. AP014541.

**Table 4**

**Generation of $F_0$ chimeric mice and their $F_1$ progeny that carry G7731A mtDNA in their tails.**

| | | 15 $F_0$ chimeric female mice | | $F_1$ mice |
|---|---|---|---|---|
| ES clones | % G7731A mtDNA | % Chimerism* | % G7731A mtDNA in tails | No. of $F_1$ pups with G7731A mtDNA / No. of $F_1$ pups |
| ESmt7731-4 | 49.8 | 95 | 68 | 4/4 |
| | | 95 | 53 | 2/12 |
| | | 90 | 45 | 24/24 |
| | | 50 | 48 | 0/17 |
| | | 40 | 16 | 0/0 |
| | | 35 | 21 | 0/8 |
| ESmt7731-7 | 48.8 | 95 | 72 | 19/19 |
| | | 95 | 76 | 4/4 |
| | | 95 | 72 | 2/12 |
| | | 95 | 68 | 8/8 |
| | | 80 | 52 | 0/8 |
| | | 60 | 61 | 0/5 |
| | | 40 | 26 | 0/0 |
| | | 15 | 13 | 0/0 |
| | | 10 | 19 | 0/0 |
| | | | | Total 63/121 |

* Chimerism was judged by coat color.

# FIGURES & LEGENDS

**Fig. 1**

**Nucleotide positions of PCR primers on the mouse mtDNA map.**

To detect small proportions of mtDNA with somatic but possibly pathogenic mutations in the $tRNA^{Leu(UUR)}$ and $tRNA^{Lys}$ genes of P29 cells, I used two sets of PCR primers so that the resultant PCR products included the $tRNA^{Leu(UUR)}$ and $tRNA^{Lys}$ genes, respectively. These products also included five additional *tRNA* genes ($tRNA^{Ile}$, $tRNA^{Gln}$, $tRNA^{Met}$, $tRNA^{Ser(CUN)}$, and $tRNA^{Asp}$).

**Fig. 1**

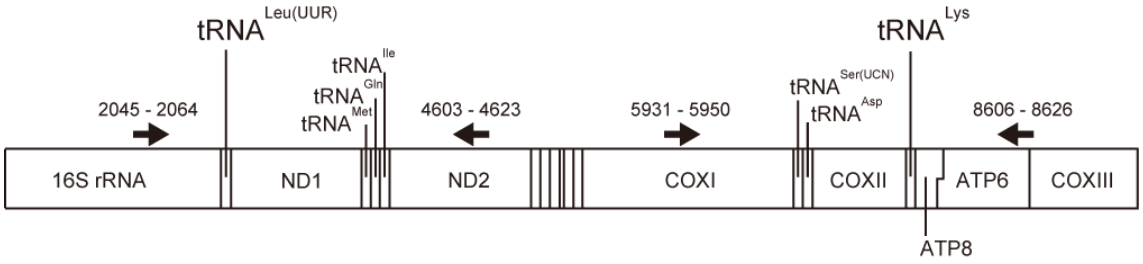
tRNA Leu(UUR)
tRNA Ile
tRNA Gln
tRNA Met
tRNA Ser(UCN)
tRNA Asp
tRNA Lys
2045 - 2064
4603 - 4623
5931 - 5950
8606 - 8626
16S rRNA
ND1
ND2
COXI
COXII
ATP6
COXIII
ATP8

**Fig. 2**

**Characterization of P29-69-183 cells to determine the pathogenicity of a G7731A mutation in the mitochondrial *tRNA*$^{Lys}$ gene.**

(A) Estimation of the proportion of G7731A mtDNA in P29 and P29-69-183 cells by *Dra*I digestion of the PCR products. The G7731A mtDNA produced 96-bp and 34-bp fragments due to the gain of a *Dra*I site through G7731A substitution in the *tRNA*$^{Lys}$ gene, whereas mtDNA without the mutation produced a 130-bp fragment. Quantitative estimation of G7731A mtDNA showed that P29-69-183 cells contained 92% G7731A mtDNA.

(B) Estimation of $O_2$ consumption rates of P29 and P29-69-183 cells.
*, $P < 0.05$.

(C) Estimation of mitochondrial superoxide levels in P29 and P29-69-183 cells after their treatment with MitoSOX Red. **, $P < 0.01$.

**Fig. 2**

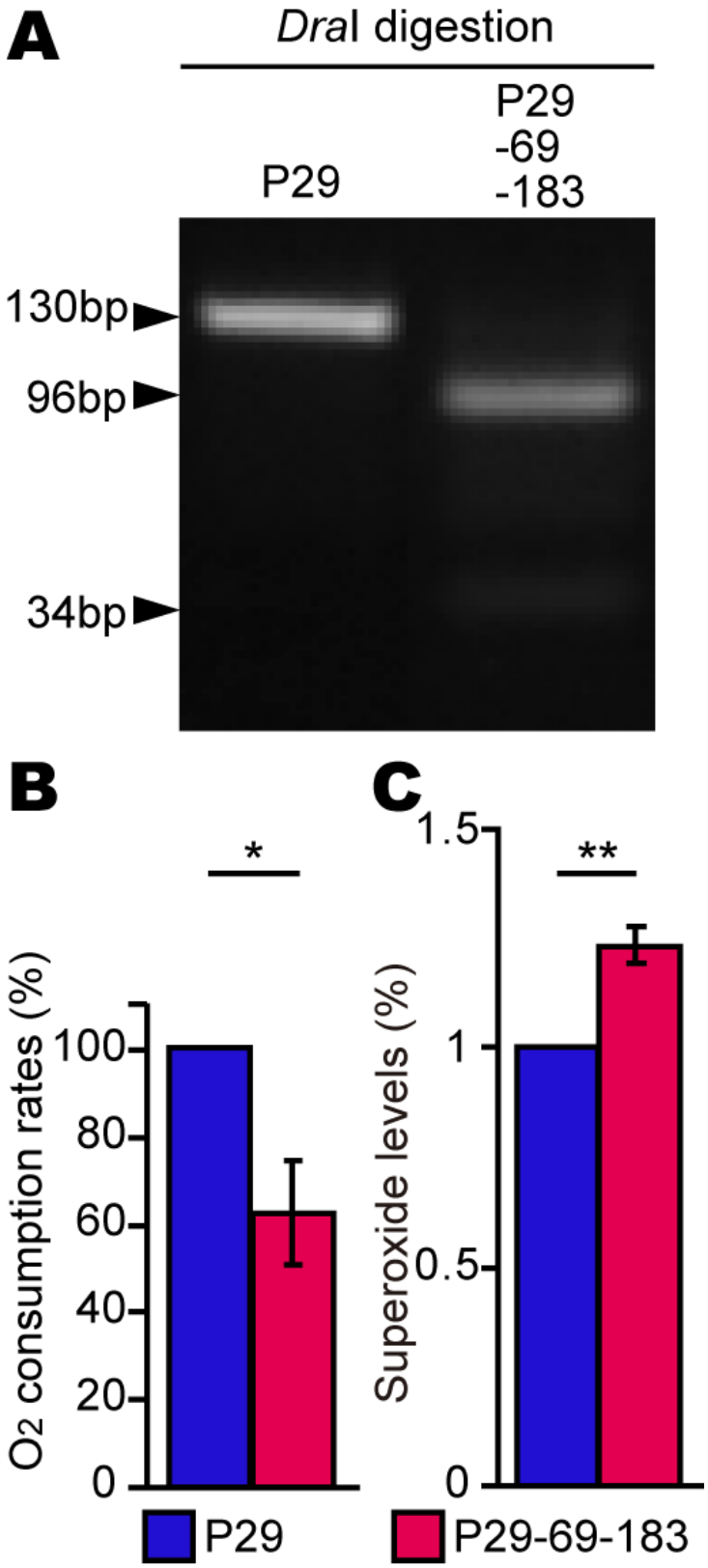
A
DraI digestion
P29
P29
-69
-183
130bp
96bp
34bp
B
C
*
**
O2 consumption rates (%)
100
80
60
40
20
0
Superoxide levels (%)
1.5
1
0.5
0
P29
P29-69-183

**Fig. 3**

**Characterization of *trans*-mitochondrial B82mt7731 cybrids for their use as G7731A mtDNA donors to ES cells.**

(A) Estimation of the proportion of G7731A mtDNA in cybrids clones B82mt7731-1 and B82mt7731-2 by *Dra*I digestion of the PCR products. Quantitative estimation of G7731A mtDNA showed that B82mt7731-1 and B82mt7731-2 had 70% and 95% G7731A mtDNA, respectively.

(B) Estimation of $O_2$ consumption rates. **, $P < 0.01$.

(C) Estimation of mitochondrial superoxide levels after treatment with MitoSOX Red. **, $P < 0.01$.

**Fig. 3**

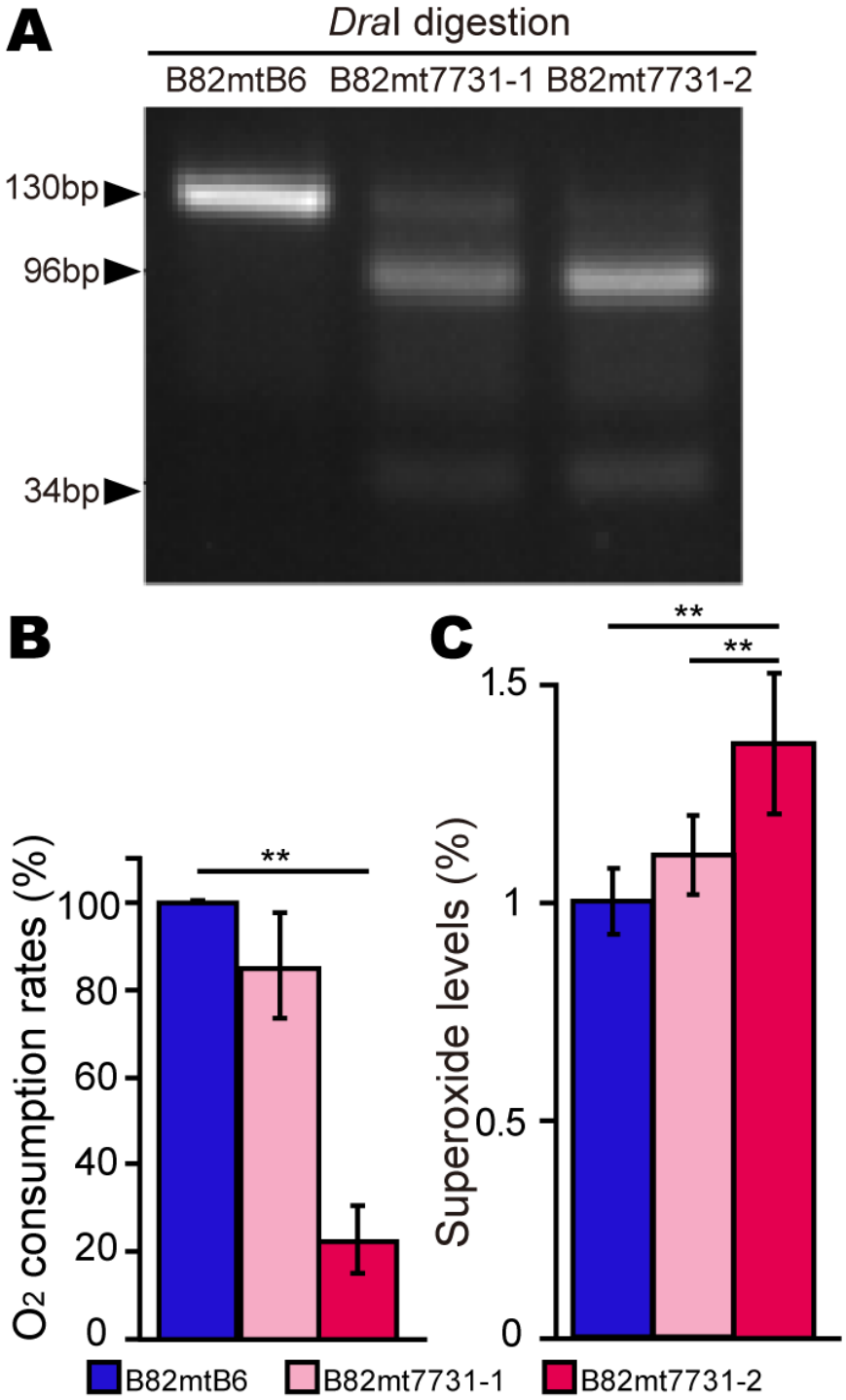
A
DraI digestion
B82mtB6
B82mt7731-1
B82mt7731-2
130bp
96bp
34bp
B
O2 consumption rates (%)
100
80
60
40
20
0
**
C
Superoxide levels (%)
1.5
1
0.5
0
**
**
B82mtB6
B82mt7731-1
B82mt7731-2

**Fig. 4**

**Identification of G7731A mtDNA in ESmt7731 cybrid clones grown in selection medium.**

I was able to obtain two ESmt7731 cybrid clones carrying G7731A mtDNA (ESmt7731-4 and -7) but was unable to exclude ES cells that lacked G7731A mtDNA, owing to incomplete elimination of endogenous mtDNA by R6G treatment. Accordingly, ESmt7731-1, -2, -3, -5, and -6 correspond to ES cells that lacked G7731A mtDNA but contained endogenous mtDNA.

**Fig. 4**

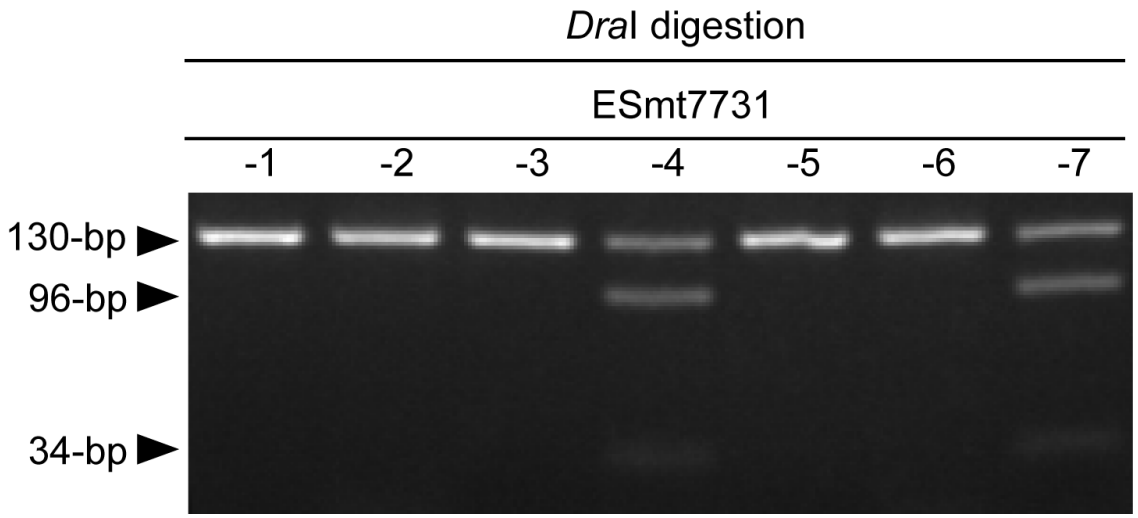

**Fig. 5**

**Variation of G7731A mtDNA proportions among pups or oocytes from individual female mice.**

(A) Variation of G7731A mtDNA proportions among $F_5$ pups born to three $F_4$ dams. G7731A mtDNA proportions were estimated by using tails from $F_5$ pups that were obtained from three $F_4$ dams with high proportions of G7731A mtDNA.

(B) Variation of G7731A mtDNA proportions among oocytes obtained from three $F_5$ female mice. G7731A mtDNA proportions were estimated by using oocytes obtained by ovarian hyperstimulation of $F_5$ female mito-mice-tRNA$^{Lys7731}$ with high proportions of G7731A mtDNA.

**Fig. 5**

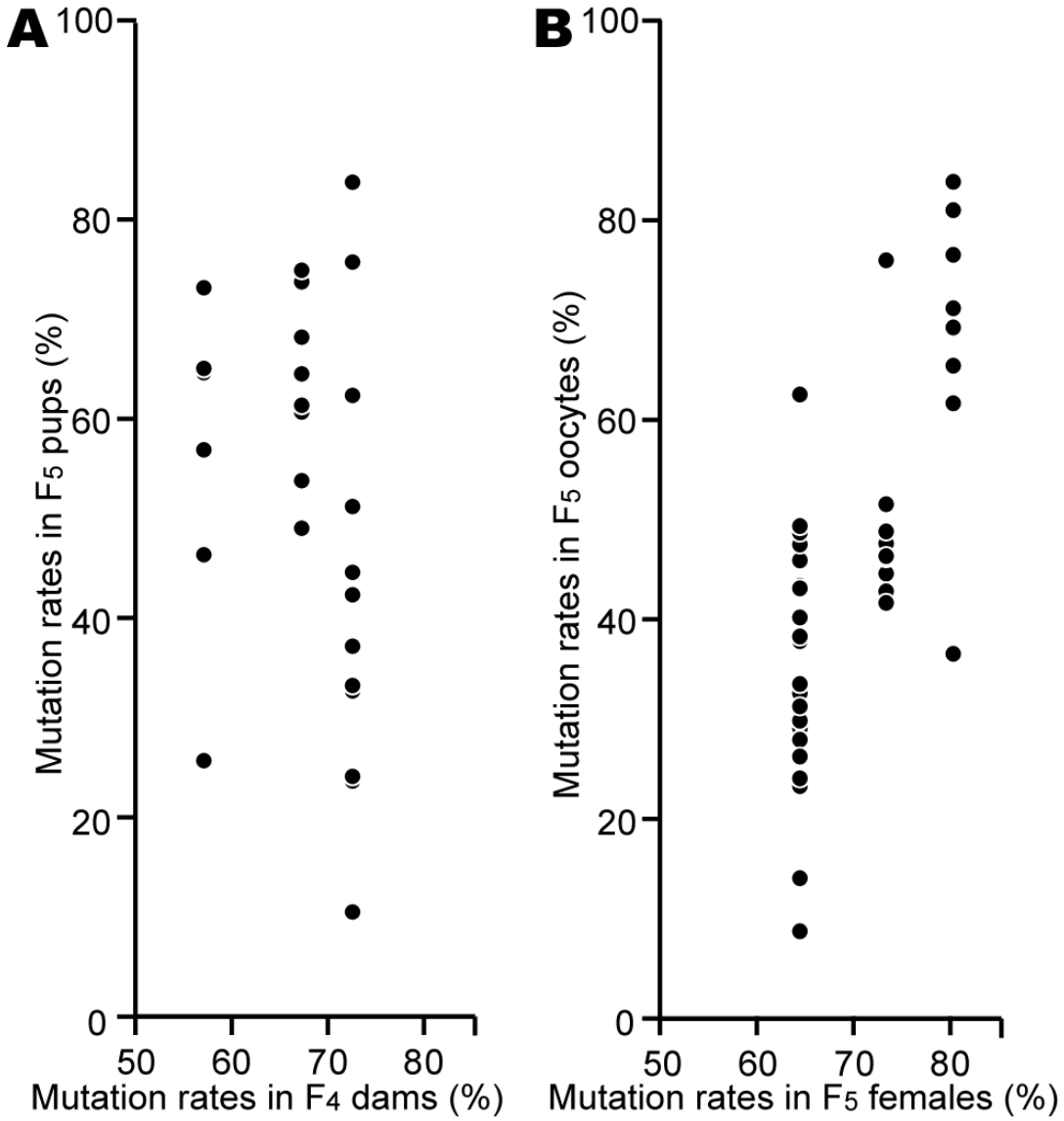
A
B
100
80
60
40
20
0
50
60
70
80
Mutation rates in F5 pups (%)
Mutation rates in F4 dams (%)
Mutation rates in F5 oocytes (%)
Mutation rates in F5 females (%)

**Fig. 6**

**Characterization of $F_5$ male mito-mice-tRNA$^{Lys7731}$ according to phenotypes associated with mitochondrial diseases.**

Comparison of (A) body length and (B) muscle (grip) strength between B6 mice (*n*=3) and $F_5$ mito-mice-tRNA$^{Lys7731}$ carrying low (13%–15%; *n* = 3), intermediate (37%–56%; *n* = 3), and high (76%–84%; *n* = 3) proportions of G7731A mtDNA. Body length and grip strength were measured at 4 months after birth. Data are presented as means ± SD. *, $P < 0.05$; **, $P < 0.01$.

(C) Comparison of activities of mitochondrial respiratory complexes (I+III, II+III, and IV) between B6 mice and $F_5$ mito-mice-tRNA$^{Lys7731}$ carrying high proportions (76–84%) of G7731A mtDNA in the skeletal muscle and the kidney at 4 months after birth. Respiratory complex I, complex II, complex III, and complex IV are components of the electron-transport chain. Enhanced activity of complex II+III in mito-mice-tRNA$^{Lys7731}$ would be due to compensatory activation of complex II, which is controlled exclusively by nuclear DNA. Data are presented as means ± SD (*n* = 3). *, $P < 0.05$; **, $P < 0.01$.

**Fig. 6**

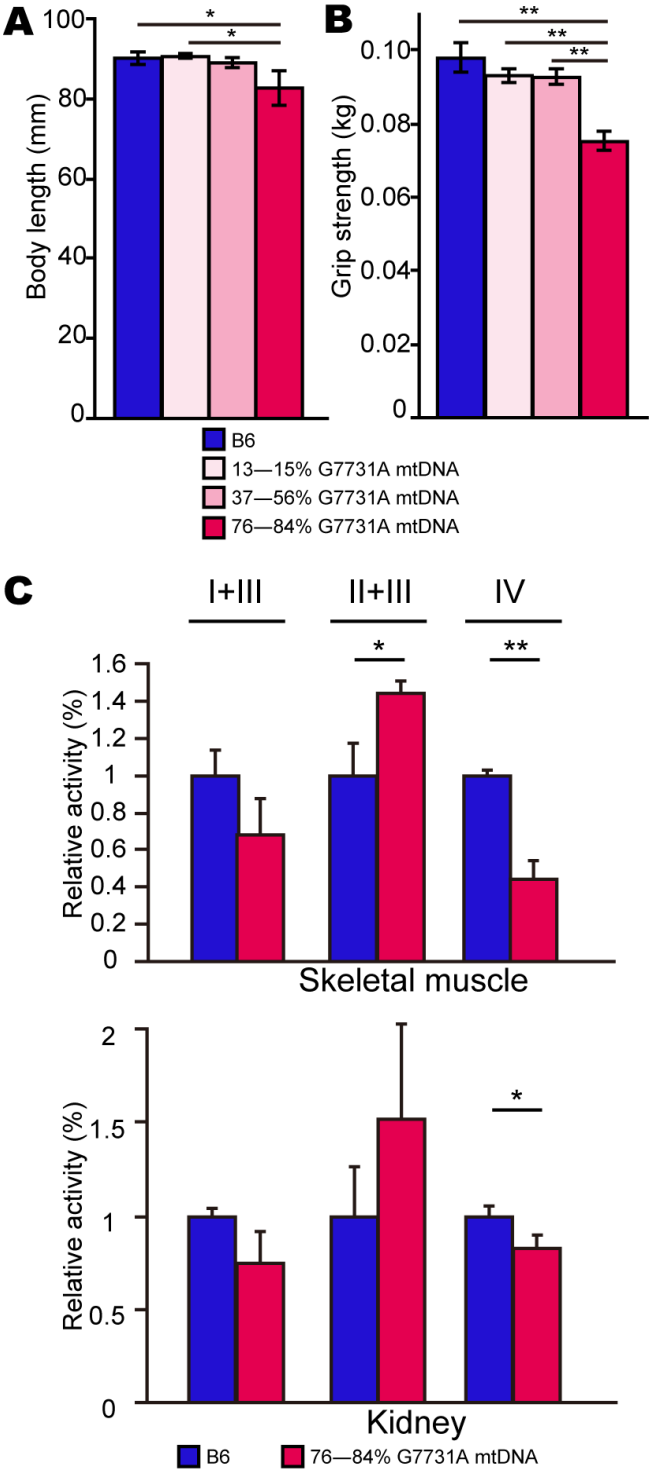
A
Body length (mm)
100
80
60
40
20
0
*
*
B
Grip strength (kg)
0.10
0.08
0.06
0.04
0.02
0
**
**
**
B6
13—15% G7731A mtDNA
37—56% G7731A mtDNA
76—84% G7731A mtDNA
C
I+III
II+III
IV
Relative activity (%)
1.6
1.4
1.2
1
0.8
0.6
0.4
0.2
0
*
**
Skeletal muscle
Relative activity (%)
2
1.5
1
0.5
0
*
Kidney
B6
76—84% G7731A mtDNA

**Fig. 7**

**Analyses of metabolic parameters related to mitochondrial diseases by using peripheral blood from mito-mice-tRNA$^{Lys7731}$ with high proportions of G7731A mtDNA.**

(A) Blood urea nitrogen.

(B) Hematocrit.

(C) Blood glucose levels before and after glucose administration.

(D) Blood lactate levels before and after glucose administration.

No statistically significant differences between B6 and mito-mice-tRNA$^{Lys7731}$ with high proportions of G7731A mtDNA were obtained. Data are presented as mean ± SD ($n$ = 3).

**Fig. 7**

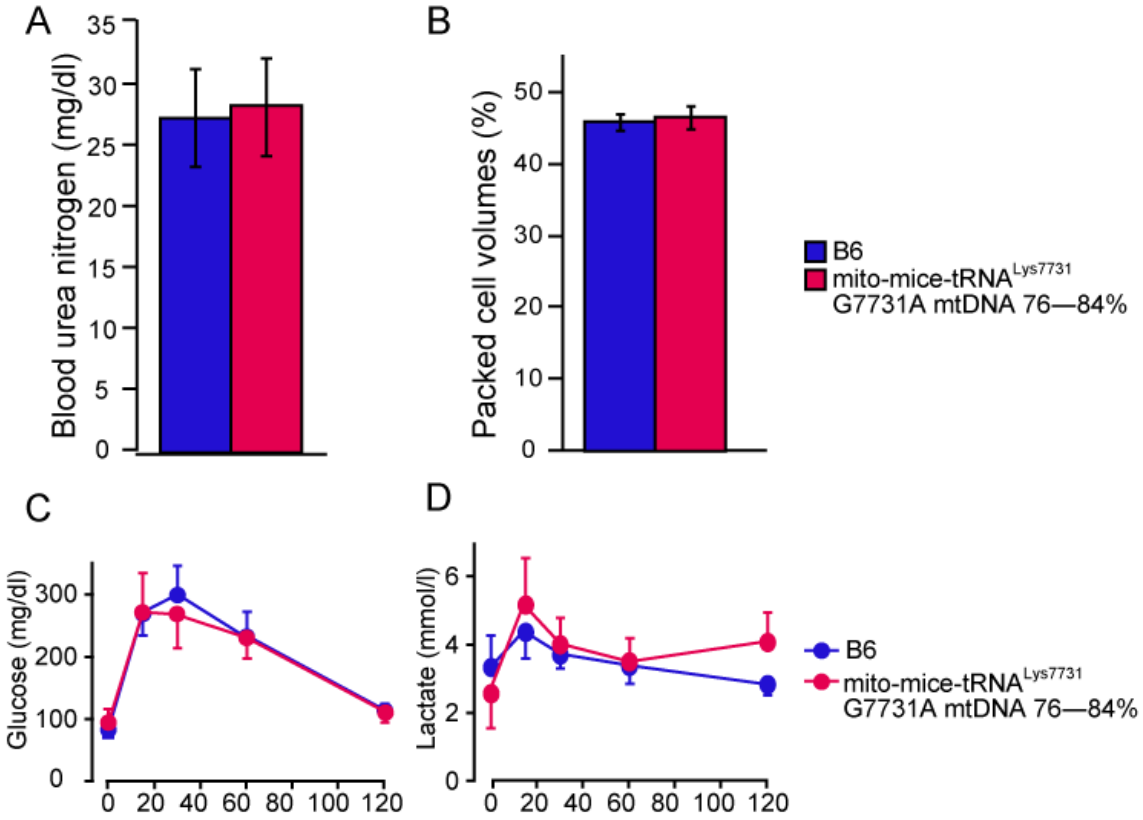
A
Blood urea nitrogen (mg/dl)
35
30
25
20
15
10
5
0
B
Packed cell volumes (%)
50
40
30
20
10
0
B6
mito-mice-tRNA Lys7731
G7731A mtDNA 76—84%
C
Glucose (mg/dl)
300
200
100
0
0 20 40 60 80 100 120
D
Lactate (mmol/l)
6
4
2
0
0 20 40 60 80 100 120
B6
mito-mice-tRNA Lys7731
G7731A mtDNA 76—84%

**Fig. 8**

**Histopathologic analysis to identify ragged red fibers (RRF) in skeletal muscle.**

Cryosections (thickness, 10 µm) of skeletal muscle were stained by using modified Gomori trichrome for histopathologic analysis to identify RRF. No RRF were present in mito-mice-$tRNA^{Lys7731}$ with high proportions of G7731A mtDNA. Bar, 50 µm.

**Fig. 8**

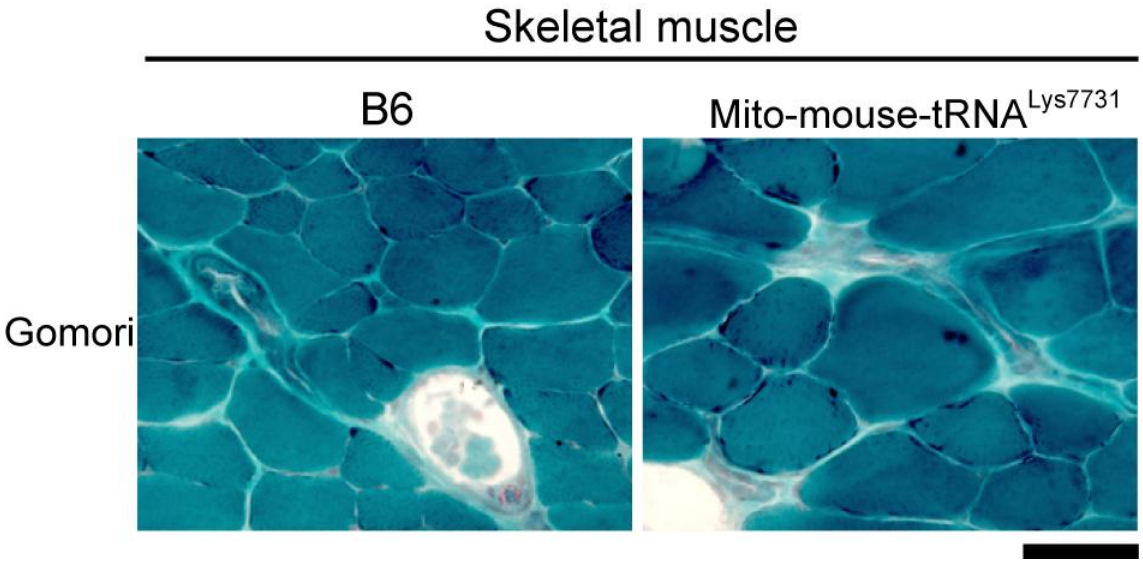

**Fig. 9**

**Morphology and histopathologic analysis of kidney.**

(A) Morphology of kidneys from B6 mouse (left) and mito-mouse-tRNA$^{Lys7731}$ with 76% G7731A mtDNA (right). Bar, 1 cm.

(B) Histopathology of the renal cortex of kidneys from B6 mice (left) and mito-mouse-tRNA$^{Lys7731}$ with 76% G7731A mtDNA (right). Formalin-fixed, paraffin-embedded sections (thickness, 5 μm) were stained with hematoxylin and eosin.

No renal failure was noted in mito-mice-tRNA$^{Lys7731}$. Bar, 50 μm.

**Fig. 9**

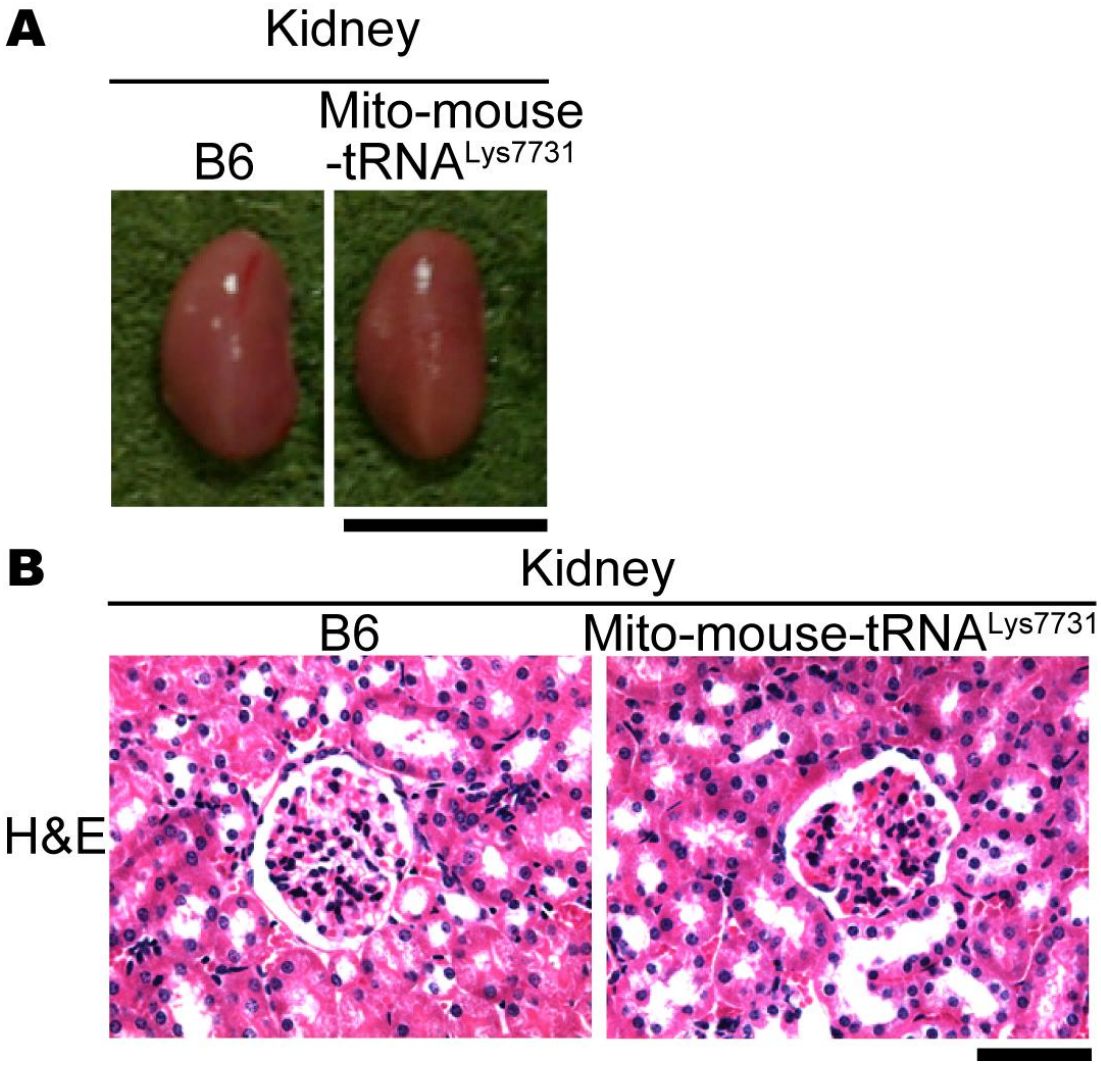
A
Kidney
B6
Mito-mouse
-tRNALys7731
B
Kidney
B6
Mito-mouse-tRNALys7731
H&E

**Fig. 10**

**Mitochondrial disease–related parameters that can be examined without euthanizing aged mito-mice-tRNA$^{Lys7731}$.**

Study populations comprised aged B6 mice (*n* = 6) and aged mito-mice-tRNA$^{Lys7731}$ with low (less than 5% in tail tissue; *n* = 4) and high (*n* = 4; 70%, 70%, 72%, and 75% in tail tissue) levels of G7731A mtDNA in tails at 4 weeks after birth. Disease-related parameters were compared at 26 months after birth.

Intergroup comparison of (A) body length, (B) grip strength, (C) hematocrit, (D) blood lactate level, (E) BUN value, and (F) blood glucose level.

Data are presented as means ±SD. *, $P < 0.05$; **, $P < 0.01$.

**Fig. 10**

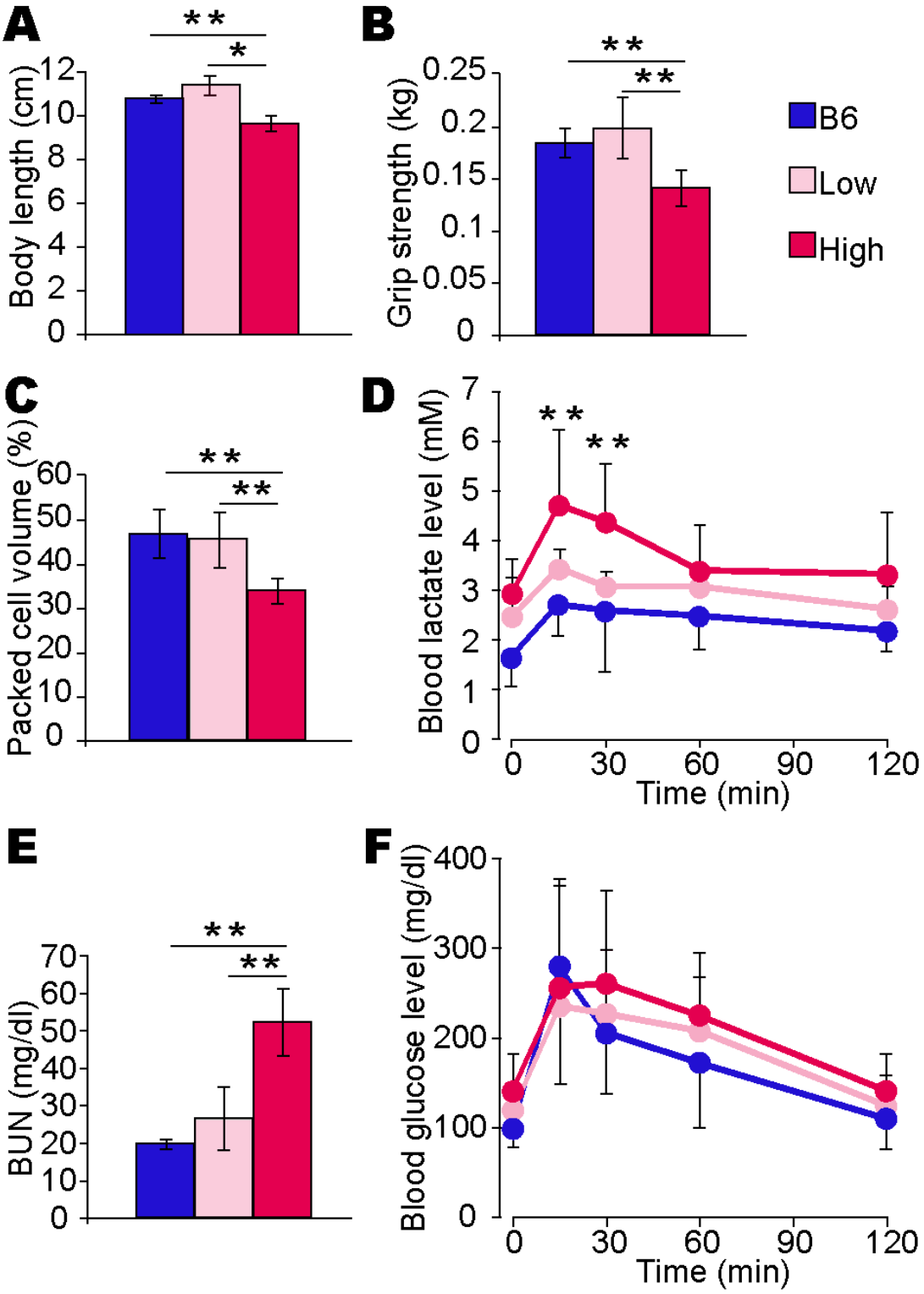
A
Body length (cm)
0
2
4
6
8
10
12
**
*
B
Grip strength (kg)
0
0.05
0.1
0.15
0.2
0.25
**
**
B6
Low
High
C
Packed cell volume (%)
0
10
20
30
40
50
60
**
**
D
Blood lactate level (mM)
0
1
2
3
4
5
6
7
**
**
0
30
60
90
120
Time (min)
E
BUN (mg/dl)
0
10
20
30
40
50
60
70
**
**
F
Blood glucose level (mg/dl)
0
100
200
300
400
0
30
60
90
120
Time (min)

**Fig. 11**

**Kaplan–Meier survival curves of B6 mice (*n* = 6) and mito-mice-tRNA$^{Lys7731}$ with low (less than 5%; *n* = 4) and high (70% to 75%; *n* = 4) levels of G7731A mtDNA.**

Median survival times were 26 months for B6 mice, 28 months for mito-mice-tRNA$^{Lys7731}$ with low levels, and 27 months for mito-mice-tRNA$^{Lys7731}$ with high levels.

**Fig. 11**

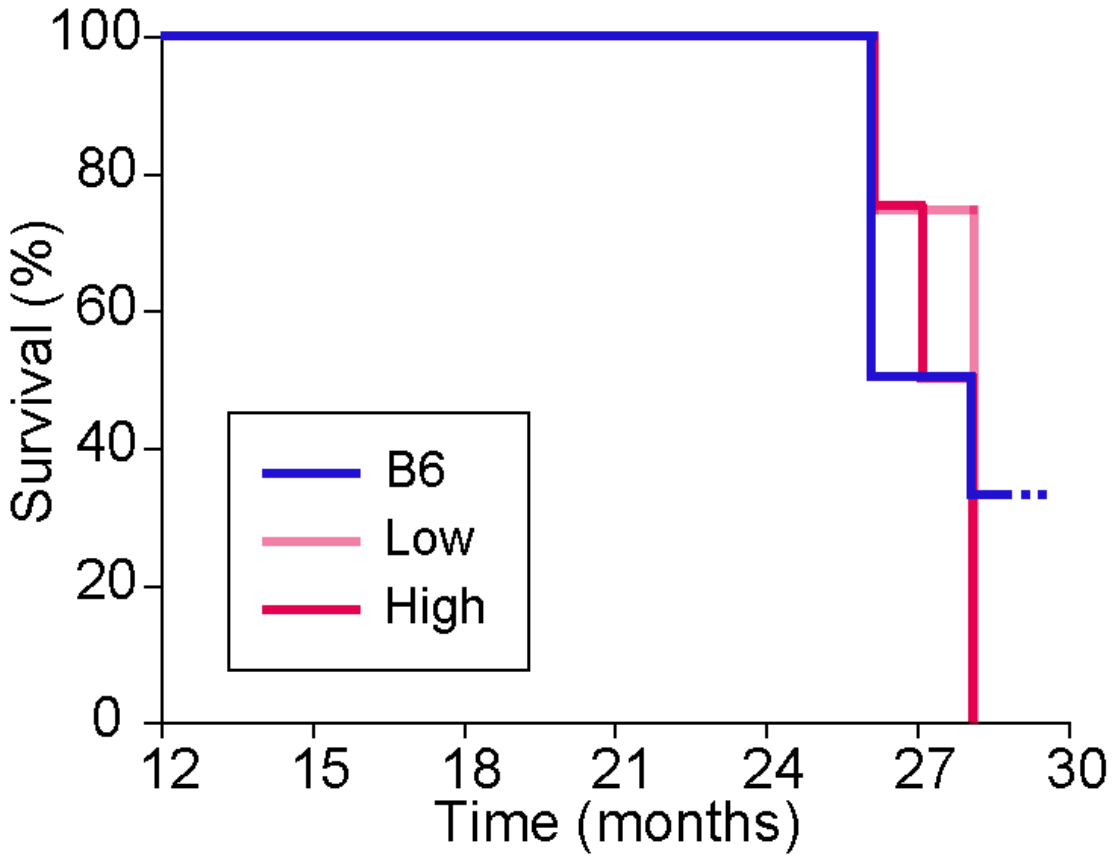
100
80
60
40
20
0
Survival (%)
B6
Low
High
12
15
18
21
24
27
30
Time (months)

**Fig. 12**

**Skeletal muscle abnormalities in aged mito-mice-tRNA$^{Lys7731}$.**

(A) Macroscopic evidence of muscle atrophy in the quadriceps of mito-mice-tRNA$^{Lys7731}$ with high levels of G7731A mtDNA. Scale bar, 5 mm.

(B) Histopathologic analysis of skeletal muscles to identify RRFs. Cryosections (thickness, 10 µm) of soleus muscle fibers were stained by using modified Gomori trichrome to identify RRFs. No RRFs were present even in aged mito-mice-tRNA$^{Lys7731}$ with high levels of G7731A mtDNA. Scale bar, 50 µm.

Genotyping of skeletal muscle (soleus) showed that the sample from the low group contained 5% G7731A mtDNA, whereas the sample from the high group contained 65% G7731A mtDNA.

**Fig. 12**

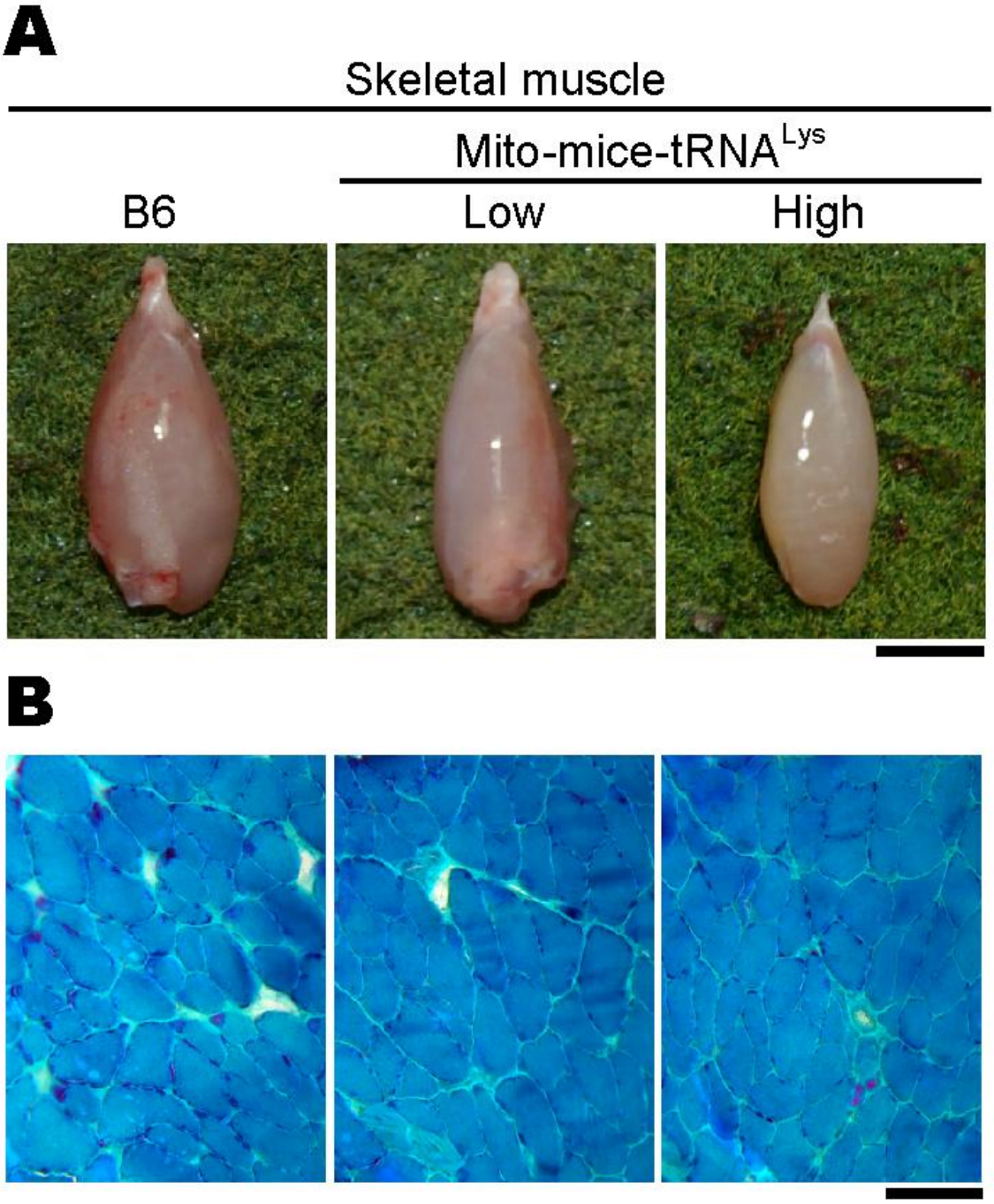

**Fig. 13**

**Renal abnormalities in aged mito-mice-tRNA$^{Lys7731}$.**

(A) Macroscopic evidence of anemic kidneys in mito-mice-tRNA$^{Lys7731}$ with high levels of G7731A mtDNA.

(B) Hemotoxylin and eosin (H&E) staining of formalin-fixed, paraffin-embedded sections (thickness, 5 μm) of renal cortex revealed dilated lumens of renal tubules and casts (arrowheads) in mito-mice-tRNA$^{Lys7731}$ with high levels of G7731A mtDNA. Scale bar, 50 μm.

(C) Histochemical analysis of mitochondrial respiratory enzyme activities in the kidney. Tissue sections were stained for COX (brown) and SDH (blue). Cells that had lost COX activity were blue because of the absence of COX activity. Scale bar, 50 μm.

Genotyping of kidney tissue showed that the sample from the low group contained 10% G7731A mtDNA, whereas the sample from the high group contained 62% G7731A mtDNA.

**Fig. 13**